

**A non-canonical melanin pathway for protection  
of *Aspergillus terreus* conidia from  
environmental stress**

Elena Geib<sup>1a,2</sup>, Markus Gressler<sup>1a</sup>, Iuliia Viediarnikova<sup>1b</sup>, Falk Hillmann<sup>1b</sup>, Ilse D. Jacobsen<sup>1c4</sup>, Sandor Nietzsche<sup>3</sup>, Christian Hertweck<sup>1d</sup> and Matthias Brock<sup>1a,2,4#</sup>

<sup>1</sup> Leibniz Institute for Natural Product Research and Infection Biology, -Hans Knoell Institute-, Beutenbergstr. 11a, 07745 Jena, Germany

<sup>a</sup> Microbial Biochemistry and Physiology

<sup>b</sup> Junior Research Group Evolution of Microbial Interactions

<sup>c</sup> Microbial Immunology

<sup>d</sup> Biomolecular Chemistry

<sup>2</sup> Fungal Genetics and Biology Group, School of Life Sciences, University of Nottingham, University Park NG7 2RD, Nottingham, UK

<sup>3</sup> Electron Microscopic Centre, University Hospital of the Friedrich Schiller University Jena, Ziegelmühlenweg 1, 07746 Jena, Germany

<sup>4</sup> Institute for Microbiology, Friedrich Schiller University, 07743 Jena, Germany

# Corresponding author

E-mail: Matthias.brock@nottingham.ac.uk

Tel.: +44 (0)115 9513315

Fax: +44 (0)115 9513251

**Running title:** Conidia pigmentation in *Aspergillus terreus*

## Abstract

Pro- and eukaryotes produce melanin for protection from environmental stress or as virulence determinant. The human pathogenic fungus *Aspergillus fumigatus* and related *Ascomycetes* produce dihydroxynaphthalene (DHN) melanin in conidia, which is essential for inhibiting phagolysosome acidification. In contrast, *Aspergillus terreus* lacks genes for biosynthesis of DHN-melanin. Therefore, the origin of the pigment in *A. terreus* conidia was elucidated. Expression analyses from conidiation conditions identified genes coding for an unusual NRPS-like enzyme (MelA) and a tyrosinase. MelA produces aspulvinone E as precursor, which is activated for polymerisation by the tyrosinase TyrP as shown by heterologous *in vivo* and *in vitro* reconstitution of pigment formation. Functional studies revealed that the pigment confers resistance against UV-light and hampers phagocytosis by soil amoeba, but does not inhibit acidification of phagolysosomes. Since *A. terreus* conidia prefer persistence at acidic pH, this uncommon type of melanin, termed Asp-melanin, might specifically contribute to survival in the environment.

## Introduction

Melanin pigments are found in all kingdoms of life and are known to protect from various environmental stress factors such as UV light or ionising radiation, oxidative and other harsh environmental conditions (Eisenman and Casadevall, 2012). In fungi, the production of melanin is very common and frequently associated with virulence. In the phytopathogen *Magnaporthe oryzae* melanisation is essential to withstand the high turgor pressure in appressoria during plant infection (Howard and Valent, 1996). In *Cryptococcus* species increased expression of melanin synthesis genes is directly associated with increased virulence (Ngamskulrungraj et al., 2011) and in *Aspergillus fumigatus* and *Penicillium marneffei* melanin increases survival in phagolysosomes, supports hydrophobin attachment to the surface of conidia and increases oxidative stress resistance (Jahn et al., 2000) (Thywissen et al., 2011) (Woo et al. (2010).

Two types of melanin are dominating in fungal species. As commonly found in mammals, some fungi produce melanin from exogenous L-3,4-dihydroxyphenylalanine (L-DOPA) or tyrosine (Eisenman and Casadevall, 2012). The second and more common type of fungal melanins results from a polyketide synthase derived naphthopyrone, which produces a dihydroxynaphthalene (DHN)-melanin. Especially in *Aspergillus* species this naphthopyrone synthase is highly conserved and mediates the inhibition of phagolysosome acidification after phagocytosis of conidia.

*Aspergillus terreus* forms an exception amongst Aspergilli as it lacks this highly conserved naphthopyrone synthase (Zachle et al., 2014); (Gressler et al., 2015b). As a consequence, *Aspergillus terreus* conidia are unable to inhibit acidification of phagolysosomes in macrophages, which results in the persistence of resting, but viable conidia in phagolysosomes (Slesiona et al., 2012a). Nevertheless, conidia of *A. terreus* display a cinnamon-brown colour, indicating that a pigment is produced for protection from biotic and

1 abiotic stress factors. However, pigment formation does not require tyrosine or L-DOPA  
2 supplementation, which implies that the pigment does not follow the melanin synthesis  
3 pathway as described for *Cryptococcus* species (Eisenman and Casadevall, 2012).  
4

5  
6 Recent investigations on secondary metabolite gene clusters indicated that a non-ribosomal  
7 peptide synthetase (NRPS)-like enzyme could be involved in *A. terreus* pigment production  
8 (Guo et al., 2015). Here, we report the discovery and characterisation of the enzymes and  
9 intermediates involved in *A. terreus* pigment synthesis and analysed the contribution of the  
10 pigment to environmental protection and virulence. Furthermore, we heterologously  
11 reconstituted pigment biosynthesis in *Aspergillus niger* and produced the pigment *in vitro*  
12 from purified enzymes. Results confirm an exceptional pigment biosynthetic pathway in  
13 conidia of the ascomycete *A. terreus* that is related to pigment biosynthesis in some  
14 basidiomycetes.  
15  
16  
17  
18  
19  
20  
21  
22  
23  
24  
25  
26  
27  
28  
29  
30

## 31 **Results**

### 32 **MelA and TyrP are required for conidia pigmentation in *Aspergillus terreus***

33  
34 We screened for secondary metabolite cluster induction during conidiation and eventually  
35 investigated the expression of all genes at locus tags ATEG\_03561-ATEG\_03570 by  
36 semiquantitative RT-PCR to identify genes that may form a pigment synthesis cluster. The  
37 *brlA* gene, known from other *Aspergilli* to regulate conidiation (Park and Yu, 2012), was  
38 selected as positive control (Fig. 1A). Genes at locus tags ATEG\_03561-03564 and  
39 ATEG\_03567-03569 showed the same expression pattern as *brlA*, whereby especially *mela*  
40 at locus tag ATEG\_03563 and the neighbouring gene ATEG\_03564, subsequently called  
41 *tyrP*, and the two genes at loci ATEG\_03567 and 03568 showed the highest expression levels  
42 (Fig. 1A). To analyse the contribution of expressed genes on pigment formation we generated  
43 the respective deletion mutants (Fig. 1B, Fig. S1A) in an *A. terreus* strain with a  $\DeltaakuB$   
44  
45  
46  
47  
48  
49  
50  
51  
52  
53  
54  
55  
56  
57  
58  
59  
60  
61  
62  
63  
64  
65

background that supports increased homologous integration rates (Gressler et al., 2011). Deletion of *mela* (ATEG\_03563) and *tyrP* (ATEG\_03564) resulted in white and bright fluorescent yellow conidia, respectively, (Fig. 1B) while none of the other mutants were affected in conidiation or pigment formation. Therefore, we hypothesised that only the NRPS-like *mela* gene and the putative tyrosinase *tyrP* are required for conidia pigment synthesis.

### **MelA produces aspulvinone E and isoaspulvinone from tyrosine**

We sequenced the full-length *mela* cDNA and identified an incorrect intron prediction. The corrected sequence contains no intron and can be found under accession number KU530117. The *mela* cDNA with or without a sequence coding for an *N*-terminal His-tag was used for transformation of *A. niger* in a recently developed high-level expression system (Gressler et al., 2015a). Regeneration of transformants on glucose (reflecting inducing condition) resulted in bright yellow fluorescent colonies with low numbers of conidia. Phenotypically normal colonies were obtained under non-inducing conditions (Fig. 1C). HPLC analyses of culture supernatants of *mela*<sup>OE</sup> strains revealed two peaks (Fig. 1D) with identical UV/Vis profiles (Fig. 1E) and molecular masses of  $m/z = 295.0611$  ( $[M-H]^-$ ) that were absent from the parental strain. This mass was in agreement with aspulvinone E (Ojima et al., 1973) with a theoretical  $m/z$  of 295.0606 ( $[M-H]^-$ ). Furthermore, NMR shifts (Fig. S1B) were in agreement with previous reports (Gao et al., 2013). One peak was identified as aspulvinone E, the second peak as its UV convertible isomer isoaspulvinone E (Gao et al., 2013) as confirmed by UV irradiation of the isolated compounds (Fig. S1C). The structure of aspulvinone E implied an origin from deaminated tyrosine and exogenous addition of tyrosine increased aspulvinone E contents in a concentration dependent manner (Fig. S1D). Therefore, 2-<sup>13</sup>C-labelled L-tyrosine was added and molecular mass analysis of purified aspulvinone E

1 indicated an exclusive labelling of two carbon atoms at defined positions (Fig. 1D) as  
2 confirmed by  $^{13}\text{C}$ -NMR analysis (Fig. S1B).  
3  
4  
5  
6

### 7 **MelA produces aspulvinone E *in vitro***

8  
9 For *in vitro* synthesis of aspulvinone E a His-tagged MelA version was purified *via* affinity  
10 chromatography on Ni-Sepharose to about 95% purity (Fig. 2A). *In vitro* analyses indicated  
11 that a slightly alkaline pH, 4-hydroxyphenylpyruvate (4-HPPA) concentrations below 10 mM  
12 and the presence of DTT appeared favourable for aspulvinone E formation (Fig. 2B). To  
13 confirm the identity of aspulvinone E and to test the substrate specificity of MelA, up scaled  
14 reactions with either 4-HPPA or phenylpyruvate as substrates were extracted and subjected to  
15 HRESI-MS-HPLC analyses. Results confirmed that aspulvinone E derives from 4-HPPA  
16 (Fig. 2C). No product was detected from phenylpyruvate (Fig. S2). These results suggest high  
17 substrate specificity of MelA, indicate a requirement for reducing conditions and show that  
18 no additional enzymes are involved in the formation of aspulvinone E from 4-HPPA.  
19  
20  
21  
22  
23  
24  
25  
26  
27  
28  
29  
30  
31  
32  
33  
34  
35

### 36 **Identification of the *tyrP* coding region**

37  
38 The *A. terreus tyrP* deletion mutant produced yellow fluorescent conidia and metabolite  
39 extraction from conidia identified aspulvinone E (Fig. 2D). Domain analyses revealed that  
40 TyrP contains a tyrosinase motif, indicating that TyrP might perform hydroxylation of  
41 aspulvinone E with subsequent oxidation as typical for this kind of enzymes (Halaouli et al.,  
42 2006). While it was possible to amplify cDNA from the predicted 3'-coding region of the  
43 *tyrP* gene, no full-length product of the predicted ORF was obtained. Subsequent cDNA  
44 sequencing revealed that the predicted ATG start codon was located within an intron  
45 sequence (Fig. 3A) and a 5'-RACE was performed. The newly derived coding region was  
46 used for a BLAST analysis against fungal proteins and a class of tyrosinase-like proteins with  
47  
48  
49  
50  
51  
52  
53  
54  
55  
56  
57  
58  
59  
60  
61  
62  
63  
64  
65

more than 50% identity to *tyrP* was detected from *Penicillium* species such as *P. expansum* (accession KGO48648), *P. camemberti* (accession CRL30472) or *P. italicum* (accession KGO71193). All sequences revealed a common export signal sequence at the *N*-terminus. Resulting from these analyses a PCR fragment spanning the proposed entire *tyrP* region was successfully amplified (accession number: KU530118). Thus, after removal of three intron sequences (Fig. 3A) the *tyrP* open reading frame codes for a protein of 356 amino acids of which the first 19 amino acids encode a putative signal sequence for cellular export as predicted by SignalP (Petersen et al., 2011).

### **TyrP induces pigment formation from aspulvinone E during heterologous expression**

The new full-length cDNA of *tyrP* was expressed with a C-terminal His-tag sequence in the *A. niger* P2 strain with or without *melA* expressing background. P2 transformants only receiving the *tyrP* gene did not show an altered phenotype. In addition, *melA* expressing *A. niger* transformants regained the ability to produce larger quantities of conidia, which might be due to a detoxification of aspulvinone E and, most strikingly, formed a dark brown coloured mycelium (Fig. 3B). To attribute pigment formation to TyrP activity, an aspulvinone E expressing *A. niger* strain was point inoculated and surrounded by *tyrP* expressing transformants (Fig. 3C). All *tyrP*-expressing strains displayed a dark brown to black non-extractable zone where mycelia of the *melA* and the *tyrP* expressing strains converged (Fig. 3C). Observation under UV light revealed that aspulvinone E fluorescence was absent from the intersection zone, while an aspulvinone E diffusion zone remained between colonies (Fig. 3C). These analyses indicate that MelA and TyrP jointly produce the *A. terreus* pigment.

### **Purification of recombinant TyrP**



For *in vitro* pigment production we aimed at purification of TyrP. Culture supernatant was collected from the *A. niger* P2 transformant *tyrP\_7* (Fig. 3C and Fig. S3), concentrated at least 100-fold and tested for pigment formation in white microplates. No activity with aspulvinone E was observed, implying that despite its *N*-terminal signal sequence TyrP is not an extracellular enzyme. On the contrary, cell-free extracts incubated with aspulvinone E led to a time dependent change in colouration and eventually disappearance of the aspulvinone E fluorescence. Although the *tyrP* gene was cloned to express a *C*-terminally His-tagged product, chromatography on Ni-Sepharose did not result in a homogenous protein band at the expected molecular mass of about 41 kDa. The majority of enzymatic activity eluted at the washing step. However, the *N*-terminal signal sequence pointed to an import into the endoplasmatic reticulum (ER) with subsequent glycosylation in the Golgi. Therefore, purification *via* ConA-agarose was performed. Strong binding of TyrP to the column was observed and up to 1.5 M  $\alpha$ -methyl-glucopyranoside were required to efficiently elute tyrosinase activity from the column. Pooled protein fractions were concentrated, desalted and subjected to chromatography on Ni-Sepharose, which resulted in a major prominent band at about 55 kDa according to SDS-PAGE analyses (Fig. 4A).

### **Glycosylation and subcellular localisation of TyrP**

Despite its apparent molecular mass of 55 kDa rather than the calculated 41 kDa mass analysis of a tryptic digest confirmed the identity of the TyrP protein. To confirm that this mass shift was due to glycosylation, periodic acid Schiff staining (PAS) of the native and denatured protein before and after deglycosylation was performed (Fig. 4B). The native protein strongly stained with PAS, whereas the denatured deglycosylated protein only stained with Coomassie and revealed a mass shift of about 15 kDa (Fig 4C). Deglycosylation of the native protein was incomplete and yielded a pattern of fully and partially deglycosylated

1 proteins. We additionally purified a full-length and *N*-terminally truncated TyrP version from  
2 *E. coli*. The deglycosylated TyrP protein matched with the *N*-terminally truncated version  
3 from *E. coli*, indicating that the signal sequence was removed during ER import (Fig 4C). To  
4 further confirm that glycosylation was not host dependent, we produced the His-tagged  
5 version of TyrP in *A. terreus*. As deduced from SDS-PAGE analyses and activity  
6 determinations the TyrP amounts from production in *A. terreus* were lower than those from  
7 the heterologous expression system in *A. niger*. However, TyrP produced in *A. terreus*  
8 revealed the same apparent molecular masses before and after deglycosylation as the protein  
9 from *A. niger* (Fig 4C).

10 To study the subcellular localisation of TyrP, a fusion with the red fluorescent protein  
11 tdTomato was produced in the *A. niger* P2 strain. The resulting reporter strains produced  
12 brown mycelium in the interaction zone with *melA*<sup>OE</sup> (Fig 4D) confirming the catalytic  
13 activity of the fusion protein. Microscopic analyses clearly indicated a subcellular localisation  
14 in granular organelles, which correlates with the predicted localisation in the ER or Golgi  
15 apparatus (Fig. 4E).

### 16 **Biochemical characterisation of TyrP**

17 Purified TyrP converted aspulvinone E *via* a blue and a greenish brown intermediate into a  
18 dark brown pigment (Video S1). Phenylthiourea (PTU) is a known inhibitor of phenol  
19 oxidases and tyrosinases (Buitrago et al., 2014); (Hall and Orlow, 2005) and approximately 2  
20 mM PTU were required to block TyrP activity (video S1 and Figure 5A). Despite a strict  
21 copper dependence of tyrosinases (Ramsden and Riley, 2014), EDTA at concentrations of up  
22 to 10 mM had no inhibiting effect on enzymatic activity (not shown). The enzyme remained  
23 active in a pH range of 4-8, but showed highest activity at pH 5-7 (Fig. 5C). Interestingly,  
24 while the aspulvinone E synthetase MelA required DTT for activity *in vitro*, TyrP activity

1 was completely inhibited in the presence of 1-2 mM DTT (Fig. 5B). This sensitivity against  
2 reducing agents correlates with the subcellular localisation in the ER and Golgi that are  
3 oxidative environments (Csala et al., 2012).  
4  
5  
6  
7  
8  
9

## 10 **Identification of TyrP reaction intermediates**

11 To analyse intermediates, TyrP reactions with aspulvinone E were extracted at different time  
12 points, evaporated, resolved in methanol and immediately subjected to LC-MS analysis.  
13  
14 Peaks for aspulvinone E rapidly declined and new peaks appeared that varied in intensity  
15 depending on time of extraction (Fig. 5D-E). Since two aromatic moieties are present in  
16 aspulvinone E, the tyrosinase should perform hydroxylations of both aromatic moieties (Fig.  
17 5F). Consistent with this hypothesis the mass of monohydroxylated aspulvinone E was  
18 detected at two different retention times (Fig. 5G). Further structure assignments were not  
19 possible due to instability of the compounds. Taking the reaction mechanisms of the di-  
20 copper centre of tyrosinases into account all modifications start with a hydroxylation in *ortho*  
21 position to the existing hydroxyl group. Its oxidation and deprotonation results in a  
22 delocalised hydroxyquinone methide anion that coincides with the blue colour initially  
23 observed in the TyrP reaction (Fig. 5C and video S1). Due to the high reactivity of methides  
24 and *ortho*-diquinones (Gill and Steglich, 1987) a polymer starts to form spontaneously that  
25 we termed Asp-melanin.  
26  
27  
28  
29  
30  
31  
32  
33  
34  
35  
36  
37  
38  
39  
40  
41  
42  
43  
44  
45  
46  
47  
48

## 49 **Impact of the conidial pigment on surface structures, biotic and abiotic stress resistance**

50 In *A. fumigatus* conidia the loss of the conidial pigment reduces the attachment of surface  
51 hydrophobins (Jahn et al., 2000). Therefore, we compared the surface structure of the  
52 parental *A. terreus*  $\DeltaakuB$  with the  $\Delta melA$  and  $\Delta tyrP$  mutants by scanning (SEM) and  
53 transmission electron microscopy (TEM) (Fig. 6A). SEM revealed a protein coating on the  
54  
55  
56  
57  
58  
59  
60  
61  
62  
63  
64  
65

1 surface of conidia from all strains. However, TEM revealed a dark zone at the outer cell wall  
2 of conidia in the wild type and the *tyrP* mutant that was lacking from the *melA* strain.  
3  
4 Resistance of *A. fumigatus* against oxidative and UV stress depends on naphthopyrone-  
5 derived pigments (Jahn et al., 2000) and Fig. S3B and S3D), but no difference in oxidative  
6 stress resistance of colour mutants was observed for *A. terreus* (Fig. S3A). However,  
7  
8 pigmentation also had a protective effect on UV resistance of *A. terreus* (Fig. 6B and S3C).  
9  
10 We then investigated the effect of pH during prolonged incubation of conidia at elevated  
11 temperature. Although the  $\Delta tyrP$  mutant showed a slightly reduced long-term survival  
12 compared to the  $\Delta melA$  mutant and the parental strain, no significant differences in pH  
13 dependent survival were observed (Fig.6C). Nevertheless, it should be noted that *A. terreus*  
14 conidia showed highest survival rates at pH 4, but were less viable when incubated at pH 7.0.  
15  
16 In contrast, conidia of other Aspergilli survived at neutral pH but were inactivated under  
17 acidic conditions (Fig. 6D). Furthermore, no significant differences were observed when  
18 mutants were tested in a chicken embryo infection model (Jacobsen et al., 2010) indicating  
19 that the pigment is of minor importance for virulence at least in this model system (Fig.6E).  
20  
21 Interestingly, when tested in a phagocytosis assay with the soil amoeba *Dictyostelium*  
22 *discoideum*, a slight, but significant reduction in phagocytosis rate was observed for the wild  
23 type compared to the pigment mutants (Fig.6F), although all strains were eventually found in  
24 acidified phagolysosomes. In summary, the pigment from *A. terreus* protects to some extent  
25 against UV light and reduces phagocytosis by amoeba.  
26  
27  
28  
29  
30  
31  
32  
33  
34  
35  
36  
37  
38  
39  
40  
41  
42  
43  
44  
45  
46  
47  
48  
49  
50

## 51 Discussion

52  
53 It has been generally assumed that filamentous ascomycetes produce DHN-melanin to protect  
54 conidia from environmental stresses (Braga et al., 2015). Our studies show that the pigment  
55  
56 in *A. terreus* conidia is unrelated to DHN-melanin. It also differs from classical eumelanins  
57  
58  
59  
60  
61  
62  
63  
64  
65

that are formed from L-DOPA. Formation of eumelanins in fungi such as *Cryptococci* relies on precursor provision from the host (Eisenman et al., 2007). In contrast, the pigment in *A. terreus* is synthesised from 4-HPPA which is converted to aspulvinone E. The biosynthesis of this Asp-melanin precursor is performed by an unusual non-ribosomal peptide synthetase-like enzyme (MelA) with a tri-domain structure consisting of an adenylation (A), thiolation (T) and thioesterase (TE) domain, but lacking the condensation domain as typical for true NRPS enzymes (Schneider et al., 2007). Some NRPS-like enzymes containing a reduction rather than a thioesterase domain have been shown to perform a substrate reduction without condensation (Wang et al., 2014). However, thioesterase containing NRPS-like enzymes mediate the condensation of two identical aromatic  $\alpha$ -keto acids and two major classes of compounds are produced: terphenylquinones and furanones (Fig. 7A) (Schneider et al., 2007), (Balibar et al., 2007), (Pauly et al., 2014), (Braesel et al., 2015), (Schuffler et al., 2011), (Brachmann et al., 2006).

The core motif of terphenylquinones is formed by two symmetric nucleophilic attacks of the C3 of one  $\alpha$ -keto acid at the C1 of the other and *vice versa* resulting in two new C-C- $\sigma$ -bonds. For formation of the butenolide core structure of furanones two divergent biosynthesis routes are possible. First, generation of a terphenylquinone intermediate, which is oxidatively cleaved and lactonised and may become decarboxylated (Schuffler et al., 2011) (Fig. 7B). Second (Pauly et al., 2014), a direct aldol condensation of two building blocks in which a single new C-C- $\sigma$ -bond is formed. This is followed by decarboxylation and lactonisation (Fig. 7C). However, different substitution patterns of the furanone core structures indicate diverging biosynthetic pathways not understood in detail yet. The furanone of aspulvinone E is substituted at positions 3 and 5, whereas it is substituted at positions 3 and 4 in ralfuranone B or 4 and 5 in xenofuranone B and allantofuranone.

Structures of aspulvinones from *A. terreus* are known since the 1970s (Ojima et al., 1973) and various models of biosynthetic pathways have been proposed. Seto (Seto, 1979) suggested a biosynthetic pathway involving atromentin as intermediate (Fig. 7B), whereas Guo et al. (Guo et al., 2015) hypothesised a direct furanone formation (Fig. 7C). However, both hypotheses were not supported by experimental data.

Recent analyses aimed at defining fingerprint motifs of the thioesterase domains that distinguish between quinone and furanone synthesis (Braesel et al., 2015). It has been assumed that quinone formation is directed by an asparagine residue present in a motif of the TE domain where it is followed by a double proline. The primary structure of MelA contains exactly this amino acid pattern, indicating a quinone product. In contrast, the labelling pattern observed from feeding 2-<sup>13</sup>C-tyrosine to *melA*<sup>OE</sup> is opposing this. The oxidative cleavage of an atromentin intermediate followed by internal ester formation would result in a randomised labelling at three positions of the molecule (Fig. 7B), but only two intensified carbon signals were found in <sup>13</sup>C-NMR spectra of aspulvinone E (Fig. 1E). Moreover, the quinone reaction pathway requires a second enzyme for oxidative opening of the terphenylquinone core, but *in vitro* biosynthesis of aspulvinone E was independent of auxiliary oxidases. Taken together, all experiments support a biosynthesis pathway as shown in Fig. 7C. Further studies are under way to analyse the amino acids that orchestrate reactions leading to either quinone or furanone core structures.

Natural products similar to the structure of aspulvinone E have been reported from basidiomycetes such as pulvinic acid derivatives like xerocomic acid in various members of the boletes (Gill and Steglich, 1987). Notably, these compounds are produced via terphenylquinone intermediates and therefore their biosynthesis significantly differs from aspulvinone E. Xerocomic and variegatic acid are monomeric compounds that give the typical yellow to red colour to some boletes mushrooms (Gill and Steglich, 1987). Bruising

1 and exposing these pigments to oxygen causes a blueing of the flesh due to the formation of  
2 delocalised hydroxyquinone methide anions (Gill and Steglich, 1987). A blue reaction  
3 intermediate was also found in the reaction of TyrP with aspulvinone E. Tyrosinases typically  
4 perform an *ortho*-hydroxylation of a mono-hydroxylated aromatic moiety followed by an  
5 oxidation leading to *ortho*-diquinones. Using high-resolution mass spectrometry the masses  
6 of such modified aspulvinone E derivatives were identified. Among these reaction  
7 intermediates we also identified a blue-coloured delocalised hydroxyquinone methide anion  
8 (Fig. 5F, structure 6a) with a marked absorption maximum at 596 nm. This anion and the  
9 *ortho*-diquinones are highly reactive intermediates that undergo auto-polymerisations leading  
10 to the brown pigment of the conidia. Interestingly, the basidiomycete *Xerocomus badius*  
11 seems to be able to suppress such a polymerisation process by producing badiones. This  
12 pigment is formed from two xerocomic acids that undergo a Diels-Alder reaction after  
13 oxidation to the diquinone without further polymerisation.  
14

15 One of the most striking questions is the reason for the lack of a DHN-melanin pigment in *A.*  
16 *terreus*. All our analyses indicate that a naphthopyrone-based pigment has superior protective  
17 effects compared to the aspulvinone-E-derived pigment from *A. terreus*. While the *A. terreus*  
18 Asp-melanin mediates UV protection, it is not protective against oxidative stress. Non-  
19 pigmented conidia reveal the same virulence as the pigmented wild type. The *A. terreus*  
20 pigment is also not involved in surface attachment of the hydrophobin layer but slightly  
21 reduces phagocytosis of conidia by amoeba. However, conidia end up in acidified  
22 phagolysosomes of macrophages (Slesiona et al., 2012a) and of *D. discoideum* as revealed  
23 from positive lysotracker staining in phagocytosis analyses. The inhibition of phagolysosome  
24 acidification, either in macrophages or other predators may depict a major function of the  
25 DHN-melanin in other *Aspergillus* species, but might be detrimental for *A. terreus*. Our  
26 analyses showed that *A. terreus* conidia survived best when incubated at pH 4, whereas  
27  
28  
29  
30  
31  
32  
33  
34  
35  
36  
37  
38  
39  
40  
41  
42  
43  
44  
45  
46  
47  
48  
49  
50  
51  
52  
53  
54  
55  
56  
57  
58  
59  
60  
61  
62  
63  
64  
65

1 conidia of *A. fumigatus*, *Aspergillus nidulans* or *A. niger* were rapidly inactivated at this pH  
2 under the applied conditions (Fig. 6). Therefore, inhibition of acidification of  
3 phagolysosomes and rapid escape are important strategies for the latter species. However,  
4 neutral pH was less well tolerated by *A. terreus* conidia. Therefore, to support a long-term  
5 persistence within phagolysosomes of predators or macrophages (Slesiona et al., 2012a);  
6  
7 (Slesiona et al., 2012b), it appears advantageous for *A. terreus* to avoid the production of a  
8 DHN-melanin that would lead to generation of less favoured environmental conditions.  
9  
10  
11  
12  
13  
14  
15  
16  
17  
18

## 19 Significance

20  
21 Bacteria, plants and vertebrates produce melanin pigments that protect from damage by UV  
22 light. Additionally, some melanins protect against oxidative stresses or increase the rigidity of  
23 the cell wall. In *Aspergillus* species a polyketide synthase produces a common melanin  
24 precursor that is polymerised to a dihydroxynaphthalene (DHN)-melanin. It has been  
25 believed that this type of melanin is generally produced by filamentous ascomycetes.  
26  
27 Nevertheless, previous studies suggested that pigment formation in *A. terreus* differs, because  
28 typical features of DHN-melanin were missing and no candidate genes for production of the  
29 naphthopyrone precursors were detectable.  
30  
31  
32  
33  
34  
35  
36  
37  
38  
39  
40

41 Herein, we identified the genes contributing to the Asp-melanin biosynthesis in *A. terreus*  
42 conidia. The pigment is produced from an NRPS-like enzyme and a tyrosinase. The NRPS-  
43 like enzyme MelA directly produces the furanone aspulvinone E, although its thioesterase  
44 domain organisation points towards the production of terphenylquinone precursor. Therefore,  
45 additional studies on the specificity of these domains are required. The tyrosinase  
46 hydroxylating and oxidising aspulvinone E is localised in subcellular organelles such as ER  
47 or Golgi, where it finds the required oxidising conditions. However, it remains speculative by  
48 which mechanism and in which form the pigment eventually locates in the cell wall of  
49  
50  
51  
52  
53  
54  
55  
56  
57  
58  
59  
60  
61  
62  
63  
64  
65



1 conidia. *A. terreus* Asp-melanin protects from UV stress and reduces phagocytosis by  
2 amoeba, but overall appears less protective than DHN melanin, raising the questions on the  
3 loss of DHN-melanin. This could be due to the preference of *A. terreus* conidia to persist  
4 within acidic environments. Unlike DHN-melanin, the *A. terreus* melanin does not inhibit  
5 acidification of phagolysosomes, which results in formation of an ecological niche that  
6 allows long-term persistence and dissemination of conidia. Therefore, the pigment produced  
7 by a specific species does not necessarily follow its phylogenetic tree rather than the need of  
8 an organism for environmental adaptation.  
9  
10  
11  
12  
13  
14  
15  
16  
17  
18  
19  
20

## 21 **Experimental procedures**

### 22 **Media and cultivation conditions**

23  
24  
25  
26 *A. niger* strains were cultivated at 28-30°C and *A. terreus* strains at 37°C. All media and  
27 strains used in this study are listed in supplemental tables. Conidia suspensions were prepared  
28 from 2% agar slants of AMM(-N)G50Gln10 medium. When required selection markers such  
29 as hygromycin B (180 µg/ml), phleomycin (80 µg/ml) or pyrithiamine (0.1 µg/ml) were  
30 added. Conidia were harvested in water, filtered through 40 µm cell strainers (Greiner,  
31 Frickenhausen, Germany), repeatedly washed in water and counted in a haemocytometer.  
32  
33 Liquid cultures were inoculated with 10<sup>6</sup> conidia/ml. For labelling experiments a 50 ml liquid  
34 AMM(-N)G50Gln10 culture of *A. niger mela*<sup>OE</sup> was supplemented with 50 mg 2-<sup>13</sup>C-L-  
35 tyrosin. For secondary metabolite extractions strains were grown in liquid media containing  
36 either 50 mM glucose or 2% starch as carbon sources. Surface biofilms for conidiation in  
37 liquid cultures were produced by incubation without shaking. *Dictyostelium discoideum* AX2  
38 was grown in cell culture dishes from frozen spores at 22 °C in 1 × HL5 or 0.2 × HL5  
39 medium (Formedium, Norfolk, UK) with 1% (w/v) glucose. Amoeba cell numbers were  
40 determined using a CASY TT Cell Counter (OLS Bio, Bremen, Germany).  
41  
42  
43  
44  
45  
46  
47  
48  
49  
50  
51  
52  
53  
54  
55  
56  
57  
58  
59  
60  
61  
62  
63  
64  
65

## RNA isolation, cDNA synthesis and semi-quantitative RT-PCR

Mycelium was ground to a fine powder and total RNA was isolated using the MasterPure RNA isolation kit (Biozym, Hess. Oldendorf, Germany). Traces of genomic DNA (gDNA) were removed with Turbo DNase (Ambion, Thermo Scientific, Braunschweig, Germany ) as confirmed by control PCR on the actin gene (ATEG\_06973) (P1/2). cDNA was synthesised by using Superscript III Reverse Transcriptase (Thermo Scientific) and anchored oligo dT primers as described previously (Zaehle et al., 2014). cDNA levels were normalised against the actin gene and used as a template for amplification of 3'-regions from secondary metabolite gene cluster genes using P5-P20 and P87-P90. Oligonucleotides are listed in the supplemental table. The *brlA* gene (ATEG\_5140) (P3/4) served as marker for conidiation.

## 5'-RACE and sequence analyses

5'-RACE was carried out on RNA of *A. terreus* with P50-P55 as described (Scotto-Lavino et al., 2006). PCR products were purified by gel electrophoresis, ligated into pJET 1.2 vectors (Thermo Scientific) and sequenced with P85 and 86. The coding sequence of the *melA* gene was analysed by sequencing genomic and cDNA with oligonucleotides P9, P10, P68, P82, P83.

## Genetic manipulation of *A. terreus* and *A. niger* and transformant analysis

Protoplast transformation of fungi was carried out as described previously (Gressler et al., 2015a; Gressler et al., 2011) using a mixture of lysing enzymes (Sigma, Taufkirchen, Germany) and yatalase (Takara Clontech, Saint-Germain-en-Laye, France). Protoplasts were regenerated on 1.2 M sorbitol containing AMM(-N)G50Gln10 media and the respective selection marker. For purification, transformants were repeatedly streaked on fresh media.

Transformants were checked by diagnostic PCR and Southern Blot analyses with digoxigenin labelled probes (Fig. S1). Blots were analysed by chemo luminescence imaging after incubation with CDP-star (Roche Diagnostics, Mannheim, Germany). Gene deletions and complementation were performed in *A. terreus* SBUG844/ $\Delta$ *akuB* (Gressler et al., 2011). In brief, 0.5 – 1 kb upstream and downstream flanks of the gene of interest were PCR amplified and fused by *in vitro* recombination (InFusion Enzyme Mix, CloneTech) with the *ptrA* resistance cassette. Complementation constructs consisted of the entire coding region including the upstream flank and a short terminator sequence, the phleomycin resistance cassette and a downstream flanking region. Fragments were assembled by *in vitro* recombination. For heterologous gene expression either the *A. niger* the P2 strain (Gressler et al., 2015a) or *A. terreus* SBUG844 was used. The standard SM-Xpress vector (Gressler et al., 2015a) or one of its His-tag versions were used for generation of heterologous expression constructs. The open reading frames of the *mela* and *tyrP* gene from *A. terreus* were amplified from cDNA. For TyrP localisation studies a fusion with the gene coding for tdTomato was generated. Oligonucleotides are shown in the supplemental table.

### Generation of a modified SM-Xpress vector set

The SM-Xpress vector was initially constructed with phleomycin as resistance marker (Gressler et al., 2015a). Here, the spectrum of cloning vectors was broadened by (i) changing the resistance marker and (ii) building a vector for introducing histidine affinity tags (His-tag). In SM-Xpress2 the phleomycin resistance cassette was replaced by the hygromycin resistance gene deleted for an internal *NcoI* restriction site, allowing transformation of strains previously transformed with the SM-Xpress vector. The *his*\_SM-Xpress vector contains a His-tag sequence that can be used adding the tag either at the C- or N-terminus of a protein.

1  
2  
3  
4  
5  
6  
7  
8  
9  
10  
11  
12  
13  
14  
15  
16  
17  
18  
19  
20  
21  
22  
23  
24  
25  
26  
27  
28  
29  
30  
31  
32  
33  
34  
35  
36  
37  
38  
39  
40  
41  
42  
43  
44  
45  
46  
47  
48  
49  
50  
51  
52  
53  
54  
55  
56  
57  
58  
59  
60  
61  
62  
63  
64  
65

Details on fragment amplification and cloning strategies are given in the supplemental experimental procedures.

### **Expression of *tyrP* in *E. coli***

For recombinant TyrP production in *E. coli* either the full-length *tyrP* (P79/P81) or a 5' truncated version (P80/P81) lacking the sequence coding for a putative export signal sequence was amplified from *A. terreus* cDNA. PCR fragments were fused with a *Bam*HI/*Hind*III restricted modified pET43.1 vector that adds an *N*-terminal His-tag to the protein (Hortschansky et al., 2007). Plasmids were propagated and re-isolated from *E. coli* DH5 $\alpha$  and transferred to *E. coli* BL21(DE3) Rosetta 2 cells (Merck, Novagen, Darmstadt, Germany) for protein production.

### **Purification of recombinant proteins**

For purification MelA and TyrP were produced with *N*- or *C*-terminal His-tag, respectively. For purification of MelA, *A. niger* P2<sub>his-melA</sub><sup>OE</sup> was grown for 26 h at 30°C in liquid YM medium. For TyrP purification, *A. niger* *tryP*<sup>OE</sup> was grown for 32 h at 28°C in AMM(-N) starch 2% Gln 50 medium and *A. terreus* *tyrP*<sup>OE</sup> for 40 h at 37° in GSMY medium (supplemental table of media), whereby for both species 10 g/l talc powder was added. Gene expression in *E. coli* was induced in Express Instant TB medium (Merck, Novagen). Fungal mycelia were disrupted by grinding under liquid nitrogen, whereas *E. coli* cells were disrupted by sonication. All His-tagged proteins were purified by Ni-chelate chromatography using Ni Sepharose 6 Fast Flow (GE Healthcare, Freiburg, Germany). For purification of TyrP an additional purification step *via* a ConA agarose (GE Healthcare) column was required. Recombinant TyrP proteins from *E. coli* were purified under denaturing conditions

from inclusion bodies. Details on specific buffers and chromatographic conditions are provided in the supplemental experimental procedures.

### **Glycostaining, deglycosylation, and MALDI-TOF MS analyses**

TyrP (60 to 100 µg) was desalted against 10 mM Tris/HCl buffer pH 7.5 (NAP5 column, GE Healthcare), lyophilised and solved in water at defined concentrations. Deglycosylation was performed under native and denaturing conditions using the protein deglycosylation mix as described in the manufacturer's protocol (New England Biolabs, Hitchin, UK). Glycostaining of proteins after SDS-PAGE on a 4-12% NuPage Bis-Tris gel was performed as described in the technical bulletin of the glycostain detection kit (Sigma-Aldrich). After extensive washings with water for enhancing band intensities the gel was photographed and subsequently stained with Coomassie R350 stain (PhastGel Blue R, GE Healthcare). For MADI-TOF MS analyses in gel tryptic digests were performed virtually as described (Shevchenko et al., 2006) using sequencing grade modified trypsin (Promega, Mannheim, Germany). Peptides were mixed with  $\alpha$ -cyano-4-hydroxycinnamic acid, dried on an MTP 800/834 anchor chip target and analysed using a Bruker Ultraflex I device (Bruker Daltonics, Bremen, Germany) as described (Teutschbein et al., 2010).

### **TyrP localisation studies**

*A. niger* producing the fusion of TyrP and tdTomato was pre-grown for 24 h on AMM(-N)Starch 2% Gln20 2% agar plates and subsequently surrounded with cover slips coated with medium solidified with 1% agar. Incubation was continued for another 24 h. Cover slips were placed on an object slide, embedded in mounting solution with DAPI (ProLong Gold Antifade with DAPI, Thermo Scientific) and covered with a large cover slip. Pictures were taken using a GXML3201LED microscope equipped with a GXCAM controlled by

1 GXCapture software (GX microscopes, Stansfield, Suffolk). Overlay images were assembled  
2 using GIMP 2 software.  
3

### 4 5 6 7 **Metabolite extraction, analysis and structure elucidation** 8

9 Metabolites were extracted from mycelium by homogenisation in ethyl acetate with an Ultra-  
10 Turrax (IKA, Staufen, Germany) at 14,000 rpm. Cell debris was removed by filtration.  
11  
12 Culture filtrates were mixed with an equal volume of ethyl acetate and the organic layer  
13 collected. Extracts were filtered over anhydrous sodium sulphate, evaporated under reduced  
14 pressure and residues solved in methanol. Analytical HPLC (Gressler et al., 2015a) and high-  
15 resolution electrospray ionisation mass spectrometry (HR-ESIMS) (Zaehle et al., 2014) were  
16 carried out as described previously. Semi-preparative isolation of aspulvinones was  
17 performed on an Agilent 1260 series equipped with DAD and quaternary pump as described  
18 in the supplemental experimental procedures. Purified metabolites were subjected to NMR  
19 analyses with DMSO-d<sub>6</sub> as solvent and internal standard. NMR Spectra were recorded either  
20 on a Bruker Avance III 500 or a Bruker Avance III 600 spectrometer (Bruker BioSpin  
21 GmbH, Rheinstetten, Germany) equipped with a cryoprobe head.  
22  
23  
24  
25  
26  
27  
28  
29  
30  
31  
32  
33  
34  
35  
36  
37  
38  
39  
40

### 41 **Aspulvinone E production and purification from recombinant MelA** 42

43 Recombinant purified MelA (10 µg) was mixed in a final volume of 20 µl with different  
44 buffers (Tris/HCl pH 8.0; potassium phosphate pH 6.2 or 6.8, PIPES pH 7.5) at a  
45 concentration of 100 mM in the presence of 5 mM ATP, 10 mM MgCl<sub>2</sub> and varying  
46 concentrations of *p*-hydroxyphenylpyruvate (0-20 mM). Also dithiotreitol (DTT) in a range  
47 of 0 to 10 mM was added. Activity was analysed by monitoring aspulvinone E fluorescence  
48 on a UV screen at 302 nm. Optimum conditions were identified as 100 mM PIPES pH 7.5  
49 with 5 mM ATP, 10 mM MgCl<sub>2</sub>, 2.5 mM DTT and 7.5 mM *p*-hydroxyphenylpyruvate. In a  
50  
51  
52  
53  
54  
55  
56  
57  
58  
59  
60  
61  
62  
63  
64  
65

10 ml scale up, 1 mg enzyme was incubated with either 7.5 mM *p*-hydroxyphenylpyruvate or 7.5 mM phenylpyruvate. Reactions without enzyme served as controls. After 18 h at 28°C, reactions were acidified to pH 3 with HCl and repeatedly extracted with ethyl acetate. Extracts were dried under reduced pressure, solved in methanol and analysed as described above.

### **TyrP *in vitro* assays and identification of TyrP reaction intermediates**

TyrP activity was assessed in 20 µl reactions by observing the time dependent pigment formation. Potassium phosphate (40 mM) at pH 6.8 in the presence of 1.8 mM aspulvinone E (from 18 mM stock solution in methanol) was used in standard analyses. Inhibitory effects of additives such as DTT, phenylthiourea or EDTA were tested in a range of 0-10 mM. Aspulvinone E consumption and pigment formation was monitored under UV and visible light at different time points. TyrP intermediates were identified from 1 ml reactions containing 5 µg TyrP, 0.61 mM Aspulvinone E and 20 mM sodium phosphate buffer pH 6.8. Samples were extracted at different time points with ethyl acetate, evaporated under reduced pressure, solved in methanol, filtered and directly injected to LC-MS on an Agilent 1260 Infinity system equipped with a quaternary pump, autosampler, diode array detector and an 6120 Quadrupole mass spectrometer in negative ionisation mode. For separation a Poroshell 120 EC-18, 4.6 × 50 mm, 2.7 µm column was used (Agilent, Waldbronn, Germany).

### **Electron microscopy**

For scanning electron microscopy conidia were collected without liquid suspension and analysed on a on a LEO-1530 Gemini field emission scanning electron microscope (Carl Zeiss NTS GmbH, Oberkochen, Germany) at electron energy of 8 keV using the in-lens secondary electron detector and 50,000 to 200,000 fold magnification. For transmission

electron microscopy conidia were harvested in sterile water and prepared for microscopy from suspension. Samples were ultrathin sectioned and analysed on an EM 900 transmission electron microscope (Carl Zeiss) at 80 kV and magnifications of 3,000 to 20,000×. Details on sample preparations can be found in the supplemental experimental procedures.

### **UV sensitivity and oxidative stress resistance of conidia**

Conidia suspensions (100 µL with  $3 \times 10^3$  conidia/ml) were plated on malt extract agar and irradiated with UV light at 254 (100 µW per cm<sup>2</sup>) nm for 10 to 60 s (Sylvania G15T8 germicidal UV-C source). The colony forming units (CFU) on control plates were set as 100 %. Each strain and time point was analysed from two independent biological replicates including three technical replicates. Oxidative stress was analysed by measuring inhibition zones in the presence of different amounts of H<sub>2</sub>O<sub>2</sub> as described in the supplemental experimental procedures.

### **Analysis of pH sensitivity and conidia germination**

Conidia were adjusted to  $6 \times 10^3$  per ml in 0.9% NaCl with 0.1% Tween 20 and mixed with an equal volume of Britton-Robinson-Buffer of different pH-values (Britton and Robinson, 1931) composed of 0.1 M of phosphoric acid, 0.1 M boric acid and 0.1 M acetic acid. Controls were plated in triplicates directly after mixing conidia with buffers and set as reference. Suspensions were incubated at 37°C for 48 h with vortex mixing every 24 h. Aliquots of 100 µl were plated in triplicates on MES buffered (25 mM, pH 6.2) malt extract agar plates. Colony forming units were determined after 24 h and 48 h of incubation at 37°C. *A. niger* was incubated at 28°C. *A. terreus* colour mutants were tested in biological replicates with technical triplicates and weighted means were calculated from both data sets. Data from other *Aspergillus* species were collected from technical triplicates. For germination analyses



conidia were labelled with fluorescein isothiocyanate (FITC) as described previously (Ibrahim-Granet et al., 2008). Conidia were incubated for 8 h in PDB medium in chamber slides and evaluated on an AxioImager fluorescence microscope (Zeiss, Jena, Germany). Details are provided in the supplemental experimental procedures.

### **Amoeba phagocytosis assay and egg infection model**

Embryonated chicken eggs were infected on the chorioallantoic membrane with  $1 \times 10^6$  conidia as described previously (Jacobsen et al., 2010); (Slesiona et al., 2012b). Survival rates were evaluated by Kaplan-Meier plots with Log-rank test. FITC-labelled conidia were used for confrontation with *D. discoideum* as described previously (Hillmann et al., 2015). After settling of amoeba for 2 h LysoTracker<sup>®</sup> Red (Fisher Scientific, Schwerte, Germany) was added in a final concentration of 100 nM. FITC stained conidia were added at an MOI of four. Microscopic images from four biological replicates were taken as tile scans of  $675 \mu\text{m}^2$  one hour post infection using an LSM 780 Live confocal laser scanning microscope (Zeiss). For each strain conidia and amoeba were counted using ImageJ software (Schneider et al., 2012). Total counts were 3248 and 807 ( $\Delta\text{akuB}$ ), 3877 and 882 ( $\Delta\text{melA}$ ), and 2191 and 715 ( $\Delta\text{tyrP}$ ) for conidia and amoeba, respectively. Phagocytosis ratio  $p_r$  was determined as previously described (Mattern et al., 2015) and defined as  $p_r = N_{phag} / (N_{phag} + N_{adh})$  with  $N_{phag}$  (phagocytosed conidia) and  $N_{adh}$  (amoeba adherent conidia). Statistical analysis was carried out using the Wilcoxon rank-sum test.

### **Authors contribution**

EG, MG, and MB conceived of and designed the experiments. EG, MG, IV, FH, IDD, SD and MB performed experiments. All authors analysed the data. EG and MB wrote the manuscript with contributions from CH and revisions were made by all authors.

## Acknowledgements

We are grateful to D. Hildebrandt and F. Meyer for general support in cloning procedures and metabolite analyses, M. Pötsch for setting up MALDI-TOF MS analyses, H. Heinicke for recording NMR spectra, A. Perner for HR-ESI-MS analyses, S. Silva and B. Weber for assistance in the chicken egg infection model and M. Samalova for valuable advice in sample preparation for fluorescence microscopy. All authors declare no conflicts of interest.

## References

- Balibar, C.J., Howard-Jones, A.R., and Walsh, C.T. (2007). Terrequinone A biosynthesis through L-tryptophan oxidation, dimerization and bisprenylation. *Nat Chem Biol* 3, 584-592.
- Brachmann, A.O., Forst, S., Furgani, G.M., Fodor, A., and Bode, H.B. (2006). Xenofuranones A and B: phenylpyruvate dimers from *Xenorhabdus szentirmaii*. *J Nat Prod* 69, 1830-1832.
- Braesel, J., Gotze, S., Shah, F., Heine, D., Tauber, J., Hertweck, C., Tunlid, A., Stallforth, P., and Hoffmeister, D. (2015). Three Redundant Synthetases Secure Redox-Active Pigment Production in the Basidiomycete *Paxillus involutus*. *Chem Biol* 22, 1325-1334.
- Braga, G.U., Rangel, D.E., Fernandes, E.K., Flint, S.D., and Roberts, D.W. (2015). Molecular and physiological effects of environmental UV radiation on fungal conidia. *Curr Genet* 61, 405-425.
- Britton, H.T.S., and Robinson, R.A. (1931). CXCVIII.-Universal buffer solutions and the dissociation constant of veronal. *Journal of the Chemical Society (Resumed)*, 1456-1462.
- Buitrago, E., Vuillamy, A., Boumendjel, A., Yi, W., Gellon, G., Hardre, R., Philouze, C., Serratrice, G., Jamet, H., Reglier, M., *et al.* (2014). Exploring the interaction of N/S

compounds with a dicopper center: tyrosinase inhibition and model studies. *Inorg Chem* 53, 12848-12858.

Csala, M., Kereszturi, E., Mandl, J., and Banhegyi, G. (2012). The endoplasmic reticulum as the extracellular space inside the cell: role in protein folding and glycosylation. *Antioxid Redox Signal* 16, 1100-1108.

Eisenman, H.C., and Casadevall, A. (2012). Synthesis and assembly of fungal melanin. *Appl Microbiol Biotechnol* 93, 931-940.

Eisenman, H.C., Mues, M., Weber, S.E., Frases, S., Chaskes, S., Gerfen, G., and Casadevall, A. (2007). *Cryptococcus neoformans* laccase catalyses melanin synthesis from both D- and L-DOPA. *Microbiology* 153, 3954-3962.

Gao, H., Guo, W., Wang, Q., Zhang, L., Zhu, M., Zhu, T., Gu, Q., Wang, W., and Li, D. (2013). Aspulvinones from a mangrove rhizosphere soil-derived fungus *Aspergillus terreus* Gwq-48 with anti-influenza A viral (H1N1) activity. *Bioorg Med Chem Lett* 23, 1776-1778.

Gill, M., and Steglich, W. (1987). Pigments of fungi (Macromycetes). *Fortschr Chem Org Naturst* 51, 1-317.

Gressler, M., Hortschansky, P., Geib, E., and Brock, M. (2015a). A new high-performance heterologous fungal expression system based on regulatory elements from the *Aspergillus terreus* terrein gene cluster. *Front Microbiol* 6, 184.

Gressler, M., Meyer, F., Heine, D., Hortschansky, P., Hertweck, C., and Brock, M. (2015b). Phytotoxin production in *Aspergillus terreus* is regulated by independent environmental signals. *eLife* 2015; 4:e07861.

Gressler, M., Zaehle, C., Scherlach, K., Hertweck, C., and Brock, M. (2011). Multifactorial induction of an orphan PKS-NRPS gene cluster in *Aspergillus terreus*. *Chem Biol* 18, 198-209.

1 Guo, C.-J., Sun, W.-W., Bruno, K.S., Oakley, B.R., Keller, N.P., and Wang, C.C.C. (2015).  
2 Spatial regulation of a common precursor from two distinct genes generates metabolite  
3 diversity. *Chemical Science* 6, 5913-5921.  
4  
5  
6  
7 Halaouli, S., Asther, M., Sigoillot, J.C., Hamdi, M., and Lomascolo, A. (2006). Fungal  
8 tyrosinases: new prospects in molecular characteristics, bioengineering and biotechnological  
9 applications. *J Appl Microbiol* 100, 219-232.  
10  
11  
12  
13  
14 Hall, A.M., and Orlow, S.J. (2005). Degradation of tyrosinase induced by phenylthiourea  
15 occurs following Golgi maturation. *Pigment Cell Res* 18, 122-129.  
16  
17  
18  
19 Hillmann, F., Novohradska, S., Mattern, D.J., Forberger, T., Heinekamp, T., Westermann,  
20 M., Winckler, T., and Brakhage, A.A. (2015). Virulence determinants of the human  
21 pathogenic fungus *Aspergillus fumigatus* protect against soil amoeba predation. *Environ*  
22 *Microbiol* 17, 2858-2869.  
23  
24  
25  
26  
27  
28  
29 Hortschansky, P., Eisendle, M., Al-Abdallah, Q., Schmidt, A.D., Bergmann, S., Thon, M.,  
30 Kniemeyer, O., Abt, B., Seeber, B., Werner, E.R., *et al.* (2007). Interaction of HapX with the  
31 CCAAT-binding complex-a novel mechanism of gene regulation by iron. *EMBO J* 26, 3157-  
32 3168.  
33  
34  
35  
36  
37  
38  
39 Howard, R.J., and Valent, B. (1996). Breaking and entering: host penetration by the fungal  
40 rice blast pathogen *Magnaporthe grisea*. *Annu Rev Microbiol* 50, 491-512.  
41  
42  
43  
44 Ibrahim-Granet, O., Dubourdeau, M., Latge, J.P., Ave, P., Huerre, M., Brakhage, A.A., and  
45 Brock, M. (2008). Methylcitrate synthase from *Aspergillus fumigatus* is essential for  
46 manifestation of invasive aspergillosis. *Cell Microbiol* 10, 134-148.  
47  
48  
49  
50  
51 Jacobsen, I.D., Grosse, K., Slesiona, S., Hube, B., Berndt, A., and Brock, M. (2010).  
52 Embryonated eggs as an alternative infection model to investigate *Aspergillus fumigatus*  
53 virulence. *Infect Immun* 78, 2995-3006.  
54  
55  
56  
57  
58  
59  
60  
61  
62  
63  
64  
65

Jahn, B., Boukhallouk, F., Lotz, J., Langfelder, K., Wanner, G., and Brakhage, A.A. (2000). Interaction of human phagocytes with pigmentless *Aspergillus* conidia. *Infect Immun* 68, 3736-3739.

Ngamskulrungrroj, P., Price, J., Sorrell, T., Perfect, J.R., and Meyer, W. (2011). *Cryptococcus gattii* virulence composite: candidate genes revealed by microarray analysis of high and less virulent Vancouver island outbreak strains. *PLoS One* 6, e16076.

Ojima, N., Takenaka, S., and Seto, S. (1973). New butenolides from *Aspergillus terreus*. *Phytochemistry* 12, 2527-2529.

Park, H.S., and Yu, J.H. (2012). Genetic control of asexual sporulation in filamentous fungi. *Curr Opin Microbiol* 15, 669-677.

Pauly, J., Nett, M., and Hoffmeister, D. (2014). Ralfuranone Is Produced by an Alternative Aryl-Substituted gamma-Lactone Biosynthetic Route in *Ralstonia solanacearum*. *J Nat Prod* 77, 1967-1971.

Petersen, T.N., Brunak, S., von Heijne, G., and Nielsen, H. (2011). SignalP 4.0: discriminating signal peptides from transmembrane regions. *Nat Methods* 8, 785-786.

Ramsden, C.A., and Riley, P.A. (2014). Tyrosinase: the four oxidation states of the active site and their relevance to enzymatic activation, oxidation and inactivation. *Bioorg Med Chem* 22, 2388-2395.

Schneider, C.A., Rasband, W.S., and Eliceiri, K.W. (2012). NIH Image to ImageJ: 25 years of image analysis. *Nat Methods* 9, 671-675.

Schneider, P., Weber, M., Rosenberger, K., and Hoffmeister, D. (2007). A one-pot chemoenzymatic synthesis for the universal precursor of antidiabetes and antiviral bis-indolylquinones. *Chem Biol* 14, 635-644.

Schuffler, A., Liermann, J.C., Opatz, T., and Anke, T. (2011). Elucidation of the biosynthesis and degradation of allantofuranone by isotopic labelling and fermentation of modified precursors. *Chembiochem* 12, 148-154.

Scotto-Lavino, E., Du, G., and Frohman, M.A. (2006). 5' end cDNA amplification using classic RACE. *Nat Protoc* 1, 2555-2562.

Seto, S. (1979). Biosynthesis of aspulvinones, metabolites from: *Aspergillus terreus*. In *Organic Chemistry*, T. Mukaiyama, ed. (Pergamon), pp. A21-A32.

Shevchenko, A., Tomas, H., Havlis, J., Olsen, J.V., and Mann, M. (2006). In-gel digestion for mass spectrometric characterization of proteins and proteomes. *Nat Protoc* 1, 2856-2860.

Slesiona, S., Gressler, M., Mihlan, M., Zaehle, C., Schaller, M., Barz, D., Hube, B., Jacobsen, I.D., and Brock, M. (2012a). Persistence *versus* escape: *Aspergillus terreus* and *Aspergillus fumigatus* employ different strategies during interactions with macrophages. *PLoS One* 7, e31223.

Slesiona, S., Ibrahim-Granet, O., Olias, P., Brock, M., and Jacobsen, I.D. (2012b). Murine infection models for *Aspergillus terreus* pulmonary aspergillosis reveal long-term persistence of conidia and liver degeneration. *J Infect Dis* 205, 1268-1277.

Teutschbein, J., Albrecht, D., Potsch, M., Guthke, R., Aimaganianda, V., Clavaud, C., Latge, J.P., Brakhage, A.A., and Kniemeyer, O. (2010). Proteome profiling and functional classification of intracellular proteins from conidia of the human-pathogenic mold *Aspergillus fumigatus*. *J Proteome Res* 9, 3427-3442.

Thywissen, A., Heinekamp, T., Dahse, H.M., Schmalzer-Ripcke, J., Nietzsche, S., Zipfel, P.F., and Brakhage, A.A. (2011). Conidial Dihydroxynaphthalene Melanin of the Human Pathogenic Fungus *Aspergillus fumigatus* Interferes with the Host Endocytosis Pathway. *Front Microbiol* 2, 96.

1 Wang, M., Beissner, M., and Zhao, H. (2014). Aryl-aldehyde formation in fungal  
2 polyketides: discovery and characterization of a distinct biosynthetic mechanism. *Chem Biol*  
3  
4 *21*, 257-263.  
5

6  
7 Woo, P.C., Tam, E.W., Chong, K.T., Cai, J.J., Tung, E.T., Ngan, A.H., Lau, S.K., and Yuen,  
8  
9 K.Y. (2010). High diversity of polyketide synthase genes and the melanin biosynthesis gene  
10 cluster in *Penicillium marneffei*. *FEBS J* 277, 3750-3758.  
11  
12

13  
14 Zaehle, C., Gressler, M., Shelest, E., Geib, E., Hertweck, C., and Brock, M. (2014). Terrein  
15 biosynthesis in *Aspergillus terreus* and its impact on phytotoxicity. *Chem Biol* 21, 719-731.  
16  
17  
18  
19  
20  
21

## 22 **Figure legends**

23  
24  
25  
26

27 **Figure 1: Cluster analysis of conidiation induced genes and heterologous expression of**  
28 ***mela*.** (A) Semi-quantitative PCR on genes of locus tags ATEG\_03561 – ATEG\_03570.  
29 cDNA was isolated from 48 h shake flask (shake) or 72 h conidiating (static) cultures from  
30 either glucose (G) or casamino acids (CA) media. Actin and *brlA* served as controls. (B)  
31 Phenotype of deletion mutants of genes (ATEG\_035XX) induced under conidiating  
32 conditions as shown in (A). Under UV light the  $\Delta tyrP$  mutant is fluorescent. (C) Comparison  
33 of an *A. niger* strain expressing the *mela* gene (*mela*<sup>OE</sup>) with the parental strain P2 on  
34 inducing glucose (G) and non-inducing casamino acids (CA) medium. (D) Metabolite  
35 extraction from P2 and *mela*<sup>OE</sup> from the culture broth of glucose medium. A dominant  
36 aspulvinone E (1) and a minor isoaspulvinone E peak (2) are visible. Feeding of 2-<sup>13</sup>C-  
37 tyrosine leads to the production of aspulvinone E exclusively labelled at positions 2 and 5 in  
38 the furanone ring (see also Fig. S1B). (E) UV/Vis spectra of aspulvinone E (1) and  
39 isoaspulvinone E (2).  
40  
41  
42  
43  
44  
45  
46  
47  
48  
49  
50  
51  
52  
53  
54  
55  
56  
57  
58  
59  
60  
61  
62  
63  
64  
65

**Figure 2: Purification and characterisation of recombinant MelA.** (A) Purification MelA from *A. niger* his\_*melA*<sup>OE</sup>. 1 = cell-free extract, 2 = flow through from Ni-NTA Sepharose, 3 = wash fraction, 4 = elution, M = molecular mass marker. (B) *In vitro* reaction of MelA in the presence of different dithiothreitol (DTT) concentrations. (C) Identification of aspulvinone E from an *in vitro* reaction of MelA with 4-hydroxyphenylpyruvate (4-HPPA) (see also Fig. S2). (D) Analysis of conidia extractions from *A. terreus* parental strain and pigment mutants. Aspulvinone E is detected only from the  $\Delta$ *tyrP* strain.

**Fig. 3: Re-identification of the *tyrP* gene and *in vivo* pigment formation.** (A) Scheme of the *tyrP* gene as previously annotated (I) and its corrected version (II). Red ATG denotes the misannotated and green ATG the experimentally verified start codon. (B) Expression of full length *tyrP* (*tyrP*<sup>OE</sup>) in the *melA* expressing background (*melA*<sup>OE</sup>) resulting in dark brown mycelium. (C) Co-cultivation of *tyrP*<sup>OE</sup> strains with the *melA*<sup>OE</sup> strain. Plates are shown in visible light as front and back view and under UV illumination in back view. Aspulvinone E produced by *melA*<sup>OE</sup> is converted into the dark brown pigment. Numbers denote independent transformants.

**Fig. 4: Purification, glycosylation and localisation of TyrP.** (A) SDS-PAGE analysis of TyrP purified from *A. niger tyrP*<sup>OE</sup>. 1 = cell-free extract, 2 = ConA column flow through, 3 = elution from ConA column, 4 = flow through from Ni-Sepharose, 5 = wash fraction, 6 and 7 = elution and concentrate from Ni-Sepharose column, M = molecular mass marker. (B) Left panel: PAS glycostain of purified untreated and deglycosylated TyrP. Right panel: Additional Coomassie stain. (C) Deglycosylation analysis of TyrP produced in *A. terreus* and *A. niger* in comparison to recombinant full-length and truncated TyrP from *E. coli*. 1 = full length TyrP *E. coli*, 2 = truncated TyrP from *E. coli*, 3 = TyrP from *A. terreus*, 4 = deglycosylated TyrP



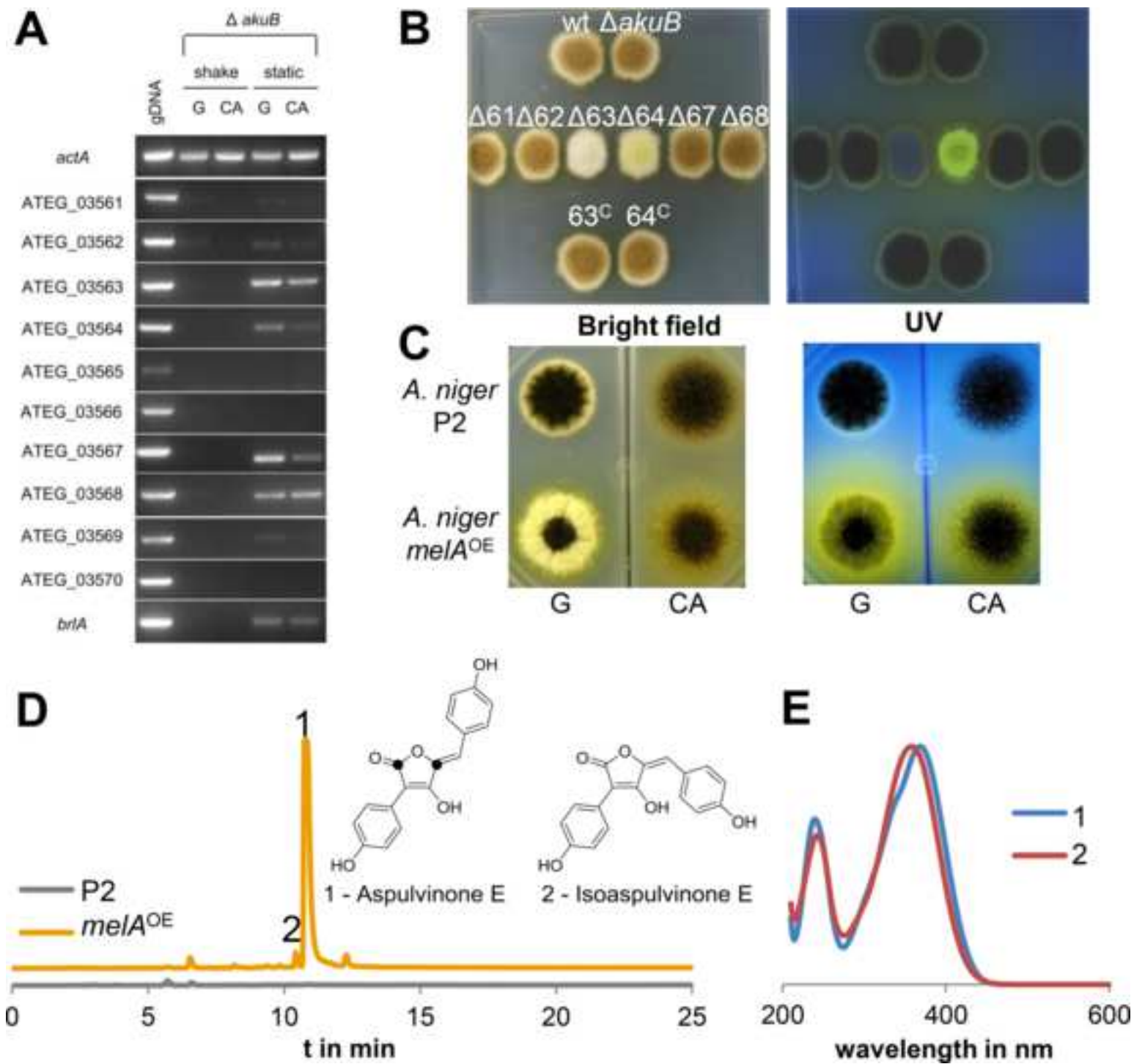
from *A. terreus*, 5 = TyrP from *A. niger*, 6 = deglycosylated TyrP from *A. niger*, 7 = native deglycosylation of TyrP from *A. niger*, M= molecular mass marker. (D) Pigmented zone formed *A. niger tyrP<sup>OE</sup>* and the *tyrP:tdTom<sup>OE</sup>* fusion strain in vicinity of *melA<sup>OE</sup>*. (E) Localisation studies of the TyrP-tdTomato fusion in *A. niger* in 200 × magnification. Bright field, tdTomato fluorescence, DAPI stain and merge are shown.

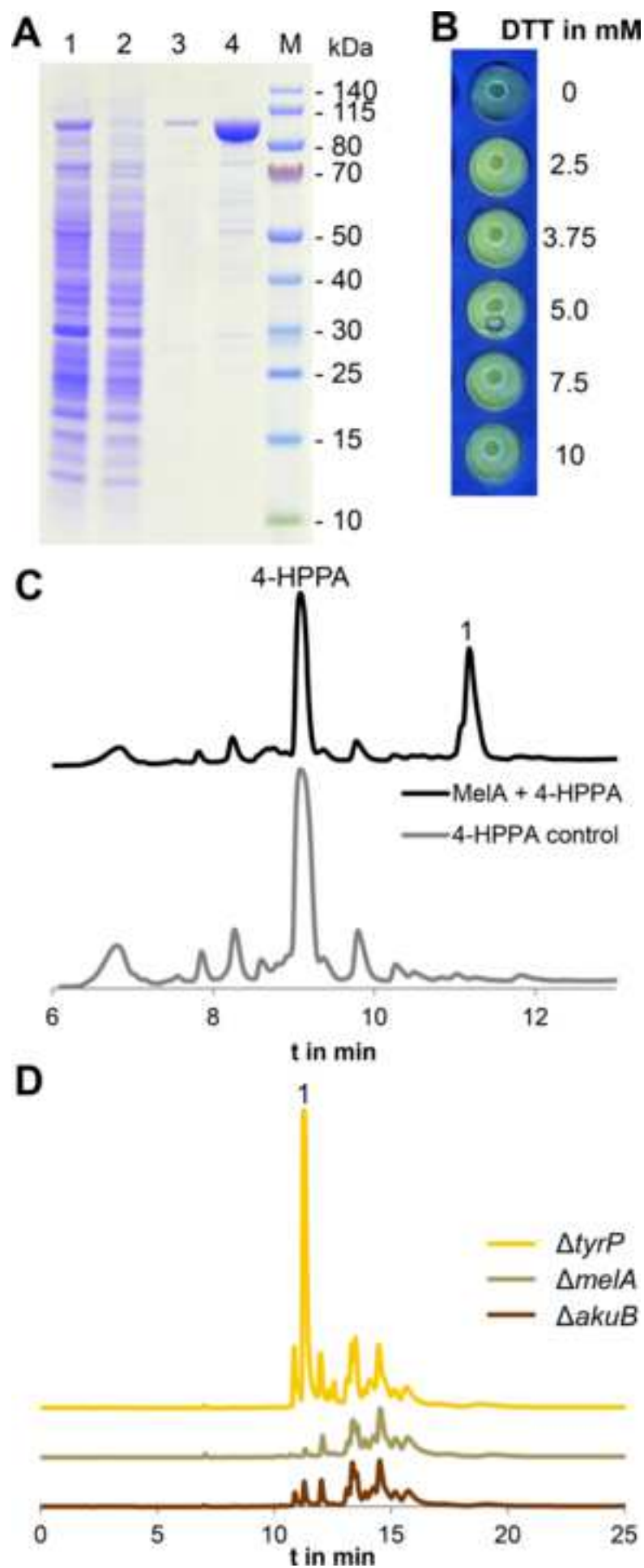
**Figure 5: Biochemical characterisation of TyrP and its reaction products.** (A) Inhibition of TyrP by different concentrations of phenylthiourea. Brown pigment formation and lack of UV fluorescence from aspulvinone E indicate TyrP activity. (B) Inhibition of TyrP by different concentrations of dithiothreitol (DTT). (C) pH dependent activity of TyrP in time lapse. (D) HPLC analysis of TyrP reaction intermediates. Aspulvinone E (1) and isoaspulvinone (2) from 0 min are rapidly converted. (E) Magnification of the HPLC profile of the TyrP reaction at 7 min with annotation of underlying structures as shown in (F) and corresponding masses as shown in (G).

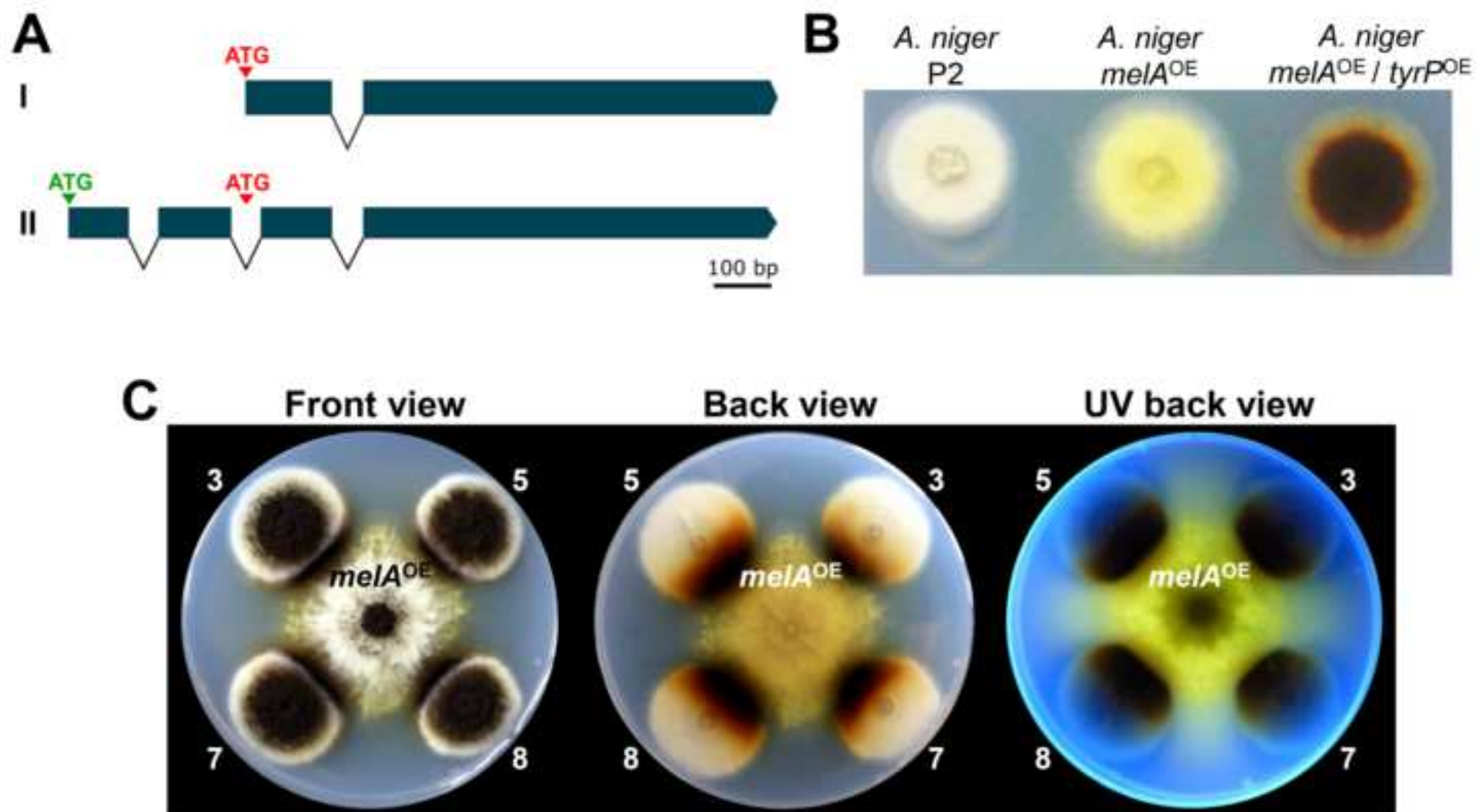
**Figure 6: Surface structure analysis and biotic and abiotic stress resistance.** (A) Scanning electron microscopic pictures (SEM) of conidia chains and detailed surface structure of single conidia. The right panel shows a transmission electron microscopy (TEM) of single conidia with a melanin layer in the wild type ( $\DeltaakuB$ ) that is less condensed in  $\Delta tyrP$  and lacking from the  $\Delta melA$  strain. Scale bars: red = 10  $\mu m$ ; yellow = 200 nm; white = 100 nm. (B) UV survival of conidia. Data from two biological replicates measured in technical triplicates are shown. Significance was calculated by student's t-test from weighted means with \*\* =  $p < 0.01$ . (C) Survival of conidia after 48 h at 37°C at different pH values. Measurements were performed in two biological replicates with technical triplicates. No statistically significant differences among strains were observed. (D) pH-dependent survival

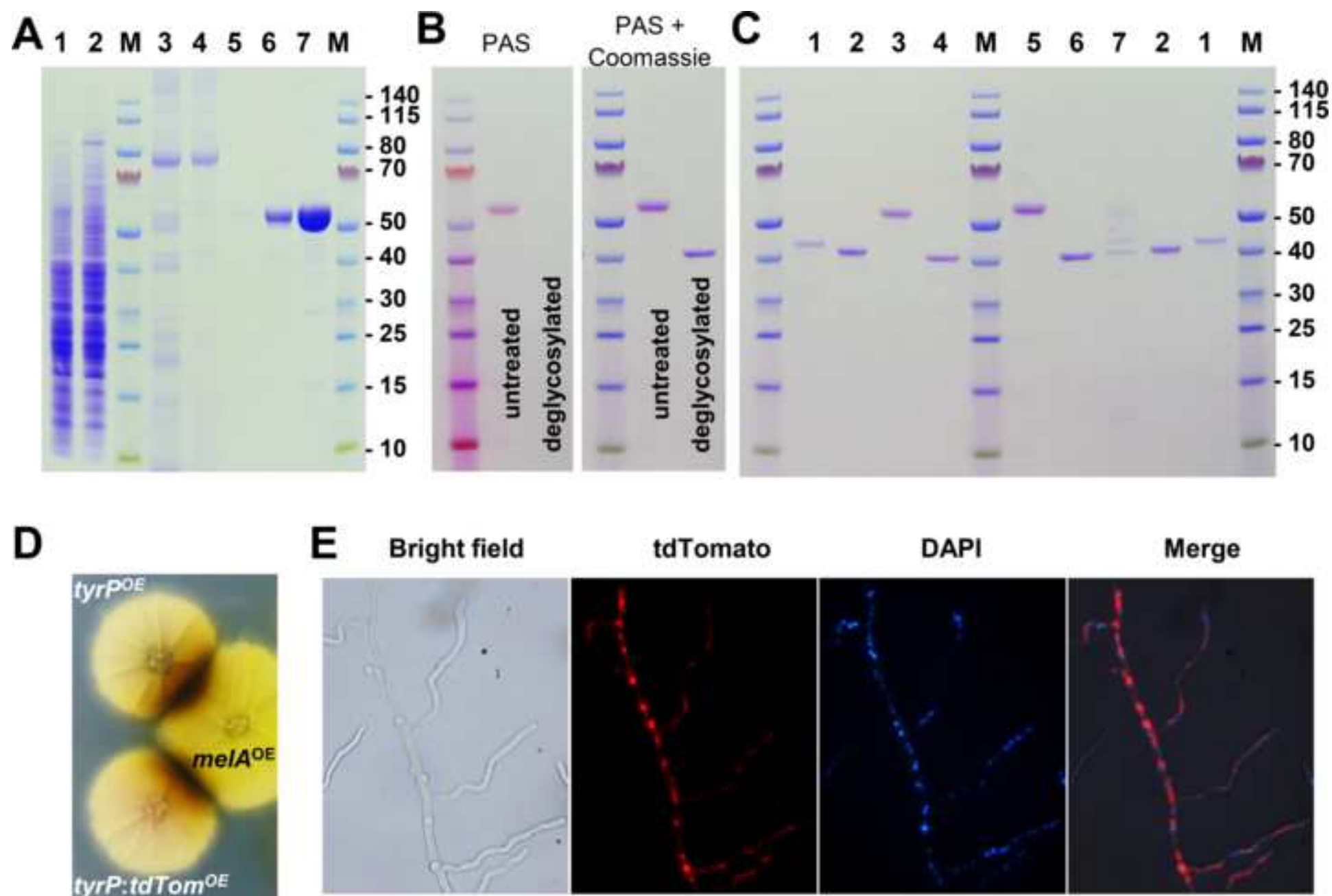
of conidia from DHN-melanin producing *Aspergillus* species and Asp-melanin producing *A. terreus* after 48 h at 37°C. Values were determined from technical triplicates. (E) Survival curve of chicken eggs infected with *A. terreus*  $\DeltaakuB$  wild type and pigment mutants. No significant differences among the three strains were observed as calculated from Kaplan Meier plots by Log-rank test. (F) Phagocytosis of conidia by *D. discoideum* amoeba. Analyses were performed from 2191-3877 conidia counts and 715-882 amoeba counts. Statistical analyses were performed by Wilcoxon rank-sum test with \* =  $p < 0.05$  and \*\* =  $p < 0.01$ . Data in B, C, D, F are shown as mean  $\pm$  SD. Further comparative analyses are shown in Fig. S3.

**Figure 7: Different NRPS-like enzyme derived metabolites and divergent pathways for biosynthesis of aspulvinone E.** (A) Core structures of terphenylquinones and furanones and selected examples for both classes of metabolites. (B) Postulated pathway for aspulvinone E biosynthesis *via* the terphenylquinone atromentin and the resulting labelling pattern when produced from 2-<sup>13</sup>C-tyrosine. (C) Biosynthesis of aspulvinone E by direct furanone formation. For details of both pathways refer to the main text. (D) Structures of xerocomic and variegatic acid and badione A from basidiomycetes.

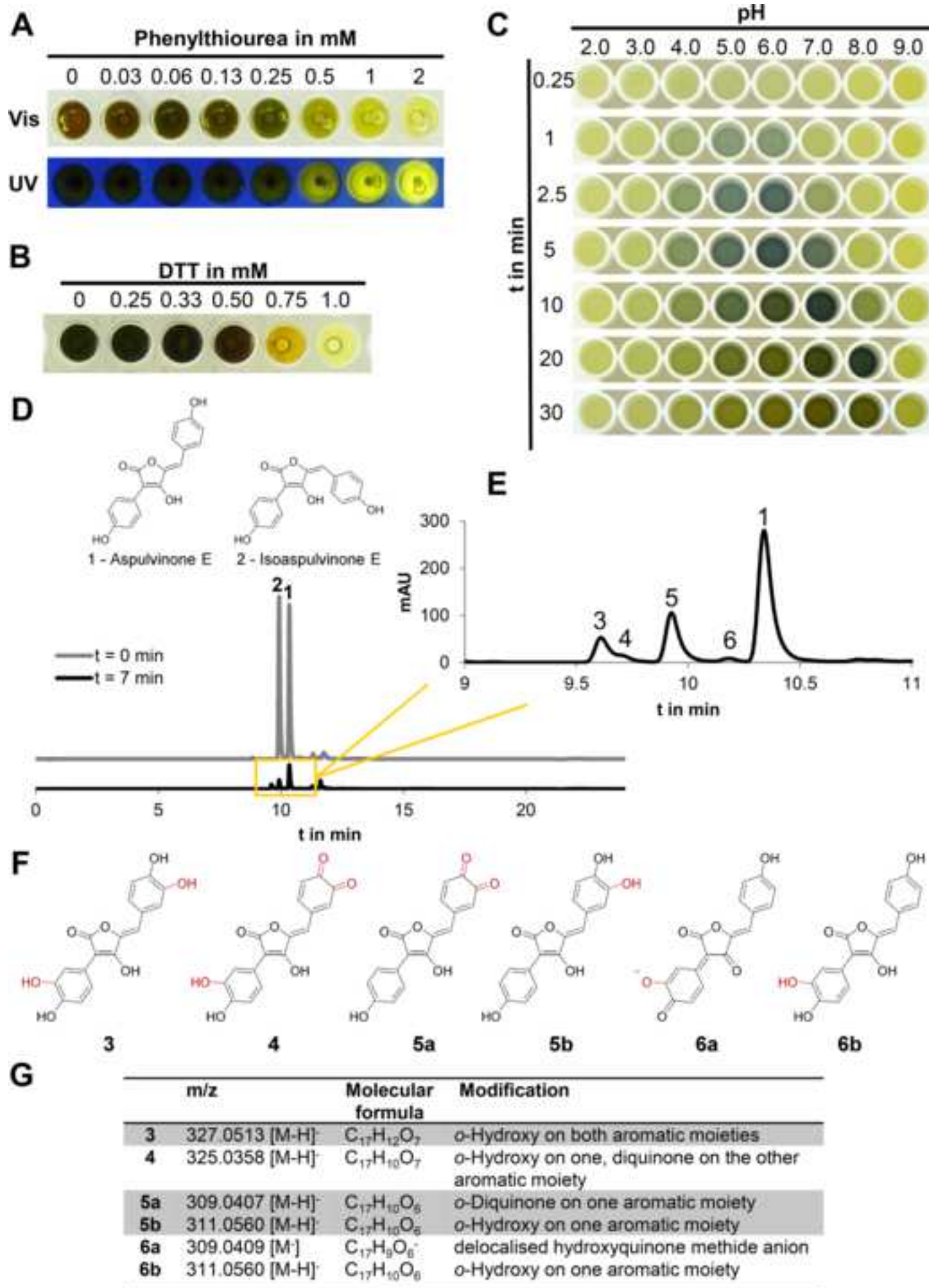


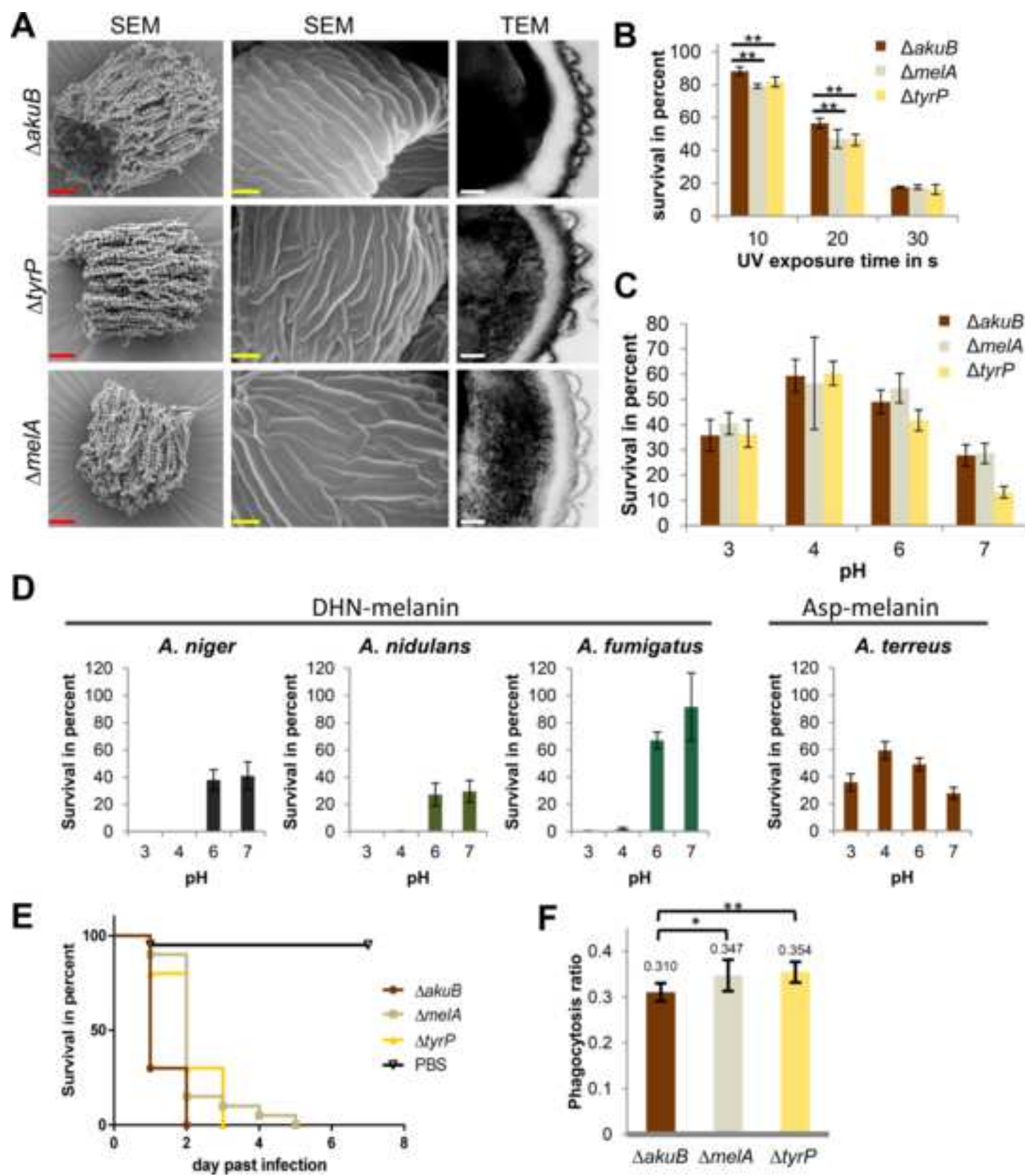




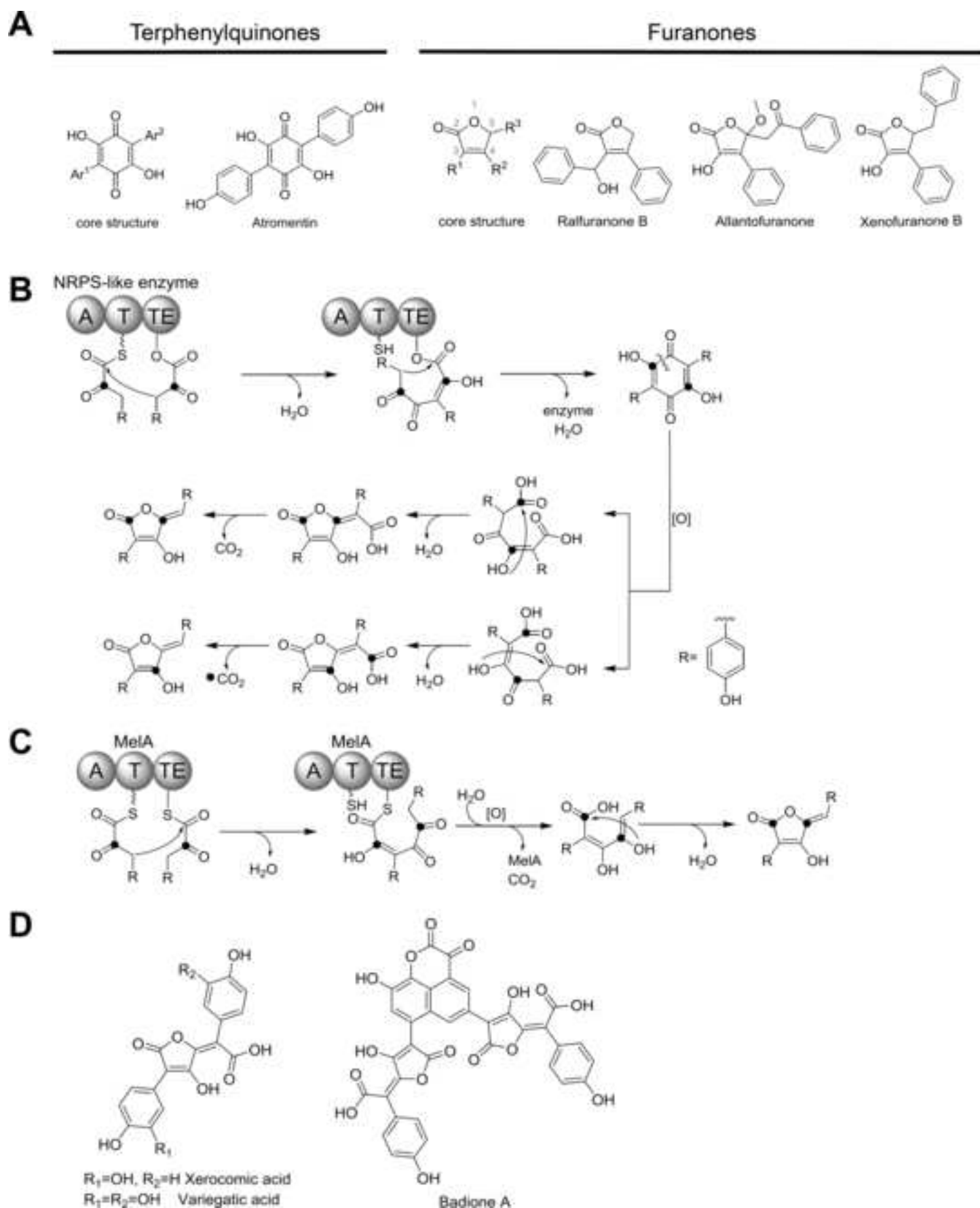














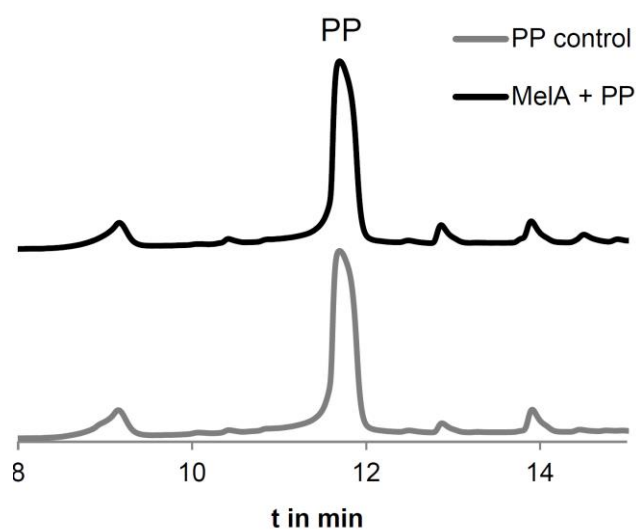


**Figure S2: Analysis of MelA reactivity on phenylpyruvate.** This figure is supplemental to Fig. 2. A 10 ml reaction with 7.5 mM phenylpyruvate and with (black line) or without (grey line) 1 mg of purified MelA was extracted and subjected to HPLC analysis. No difference between both samples is observed, indicating that MelA does not use phenylpyruvate as substrate.

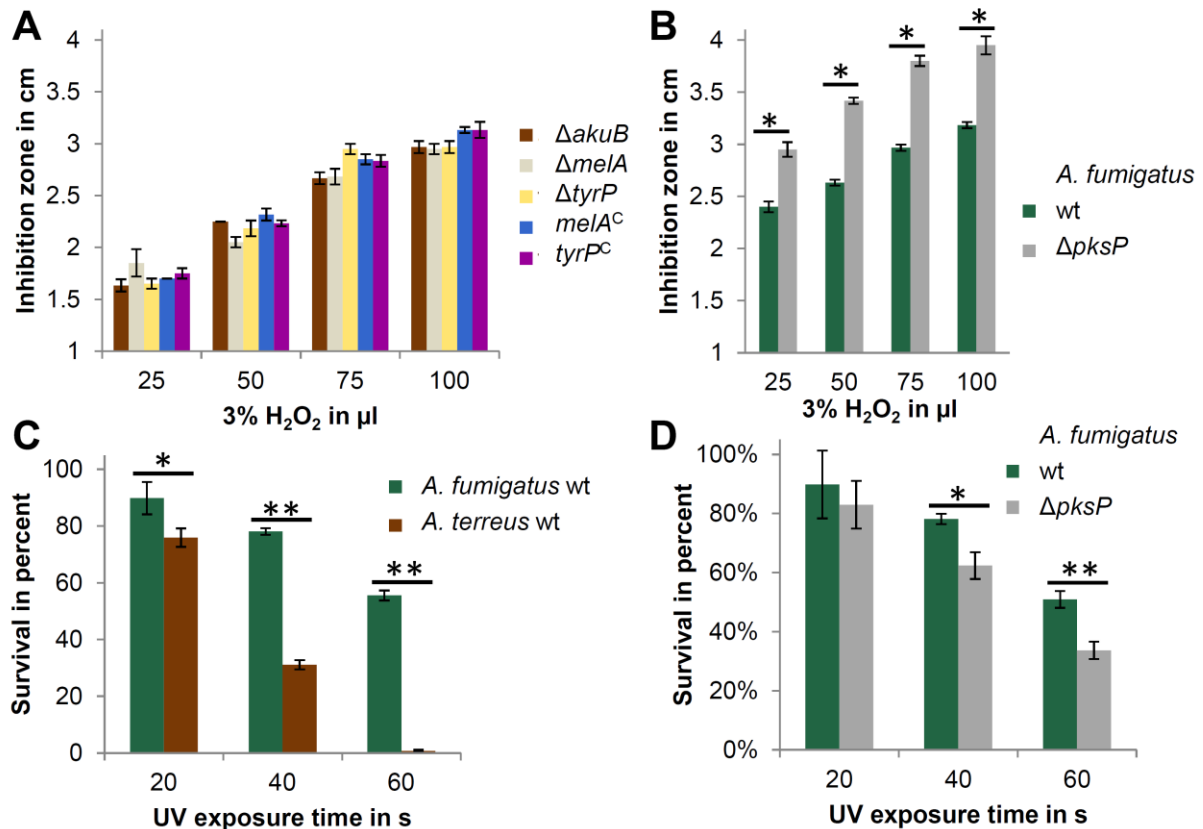


**Figure S3: Oxidative and UV stress resistance of *A. terreus* and *A. fumigatus* wild type and mutant strains.** This figure is supplemental to Fig. 6. **(A)** Sensitivity of *A. terreus*  $\Delta akuB$  wild type, pigment mutants and complemented strains against hydrogen peroxide. No significant differences in diameters of inhibition zones were observed. **(B)** Same analysis as in (A), but with *A. fumigatus* wild type and corresponding white *pksP* mutant. **(C)** Comparison of *A. fumigatus* and *A. terreus* wild type strains (without genetic  $\Delta akuB$  background). *A. fumigatus* appears naturally more UV resistant than *A. terreus*. **(D)** UV sensitivity of *A. fumigatus* wild type and corresponding white *pksP* mutant. The wild type shows increased UV protection. All data were collected from biological duplicates performed in technical triplicates. Significance was calculated by student's t-test from weighted means with \*= $p < 0.05$  and \*\*= $p < 0.01$ . Data are shown as mean  $\pm$  SD.

### Supplemental video information

**Video S1: Recording of the *in vitro* reaction of TyrP with and without tyrosinase inhibitor.** This video is supplemental to Fig. 5. A 96-well microplate with total reaction volumes of 20  $\mu$ l was used for recording the TyrP reaction in a time-lapse movie. The movie shows for wells. Upper left = aspulvinone E control without TyrP. Upper right = TyrP with 2 mM of the tyrosinase inhibitor phenylthiourea (PTU). Lower left = aspulvinone E with TyrP. Lower right = aspulvinone E with 2 mM PTU and TyrP. Over a total period of 60 min single photographs were taken every 20 s under magnification of a Leica S8APO Binocular equipped with a QImaging MicroPublisher 3.3 RTV camera. Pictures were assembled with Image-Pro Insight (Media Cybernetics Software). Due to technical reasons, the first two min after starting the reaction with TyrP have not been recorded.

## Supplemental Tables

**Table of oligonucleotides used in this study.** This table is supplemental to the experimental procedures and is provided as a separate Excel file.

**Table of media used in this study.** This table is supplemental to the experimental procedures.

Minimal media	
AMM	6 g/l NaNO <sub>3</sub> , 0.52 g/l KCl, 0.52 g/l MgSO <sub>4</sub> × 7 H <sub>2</sub> O, 1.52 g/l KH <sub>2</sub> PO <sub>4</sub> ; 1 ml/l 1000× Hutner's trace elements (Hutner et al., 1950); pH 6.5
G50	50 mM glucose
G100	100 mM glucose
AMM(-N)	0.52 g/l KCl, 0.52 g/l MgSO <sub>4</sub> × 7 H <sub>2</sub> O, 1.52 g/l KH <sub>2</sub> PO <sub>4</sub> ; 1 ml/l 1000× Hutner's trace elements; pH 6.5
G50Gln20	50 mM glucose and 10 mM glutamine
CA1%	1% casamino acids
Starch2%Gln50	2% starch and 50 mM glutamine
Complex media	
YM	3 g/l yeast extract, 3 g/l malt extract, 5 g/l meat peptone; pH 6.6
GSMY	30 g/l glucose, 2.5 g/l soy bean meal, 0.5 g/l yeast extract, 1 g/l KH <sub>2</sub> PO <sub>4</sub> , 1 g/l MgSO <sub>4</sub> × 7 H <sub>2</sub> O, 0.5 g/l NaCl, 0.5 g/l CaCl <sub>2</sub> × 2 H <sub>2</sub> O, 2 mg /l FeCl <sub>3</sub> × 2 H <sub>2</sub> O, 2 mg/l ZnSO <sub>4</sub> × 7 H <sub>2</sub> O; pH 5.5
PDB	24 g/l potato dextrose broth, pH 6.5
Malt agar	30 g malt extract, 5 g bacterial peptone, 2% agar

**Table of strains used in this study.** This table is supplemental to the experimental procedures.

Strain	Genotype	Reference
<i>A. terreus</i> SBUG844		JMRC; HKI; Jena
<i>A. terreus</i> $\Delta$ akuB	<i>A. terreus</i> SBUG 844 $\Delta$ akuB::hph <sup>R</sup>	Gressler et al., 2011
<i>A. terreus</i> $\Delta$ melA	<i>A. terreus</i> SBUG 844 $\Delta$ akuB::hph <sup>R</sup> ; $\Delta$ melA::ptrA <sup>R</sup>	this study
<i>A. terreus</i> $\Delta$ tyrP	<i>A. terreus</i> SBUG 844 $\Delta$ akuB::hph <sup>R</sup> ; $\Delta$ tyrP::ptrA <sup>R</sup>	this study
<i>A. terreus</i> $\Delta$ 03561	<i>A. terreus</i> SBUG 844 $\Delta$ akuB::hph <sup>R</sup> ; $\Delta$ 03561::ptrA <sup>R</sup>	this study
<i>A. terreus</i> $\Delta$ 03562	<i>A. terreus</i> SBUG 844 $\Delta$ akuB::hph <sup>R</sup> ; $\Delta$ 03562::ptrA <sup>R</sup>	this study
<i>A. terreus</i> $\Delta$ 03567	<i>A. terreus</i> SBUG 844 $\Delta$ akuB::hph <sup>R</sup> ; $\Delta$ 03567::ptrA <sup>R</sup>	this study
<i>A. terreus</i> $\Delta$ 03568	<i>A. terreus</i> SBUG 844 $\Delta$ akuB::hph <sup>R</sup> ; $\Delta$ 03568::ptrA <sup>R</sup>	this study
<i>A. terreus</i> tryP <sup>OE</sup>	<i>A. terreus</i> SBUG844; AtPterA:tyrP:AttrpC <sup>T</sup>	this study
<i>A. niger</i> A1144		FGSC; Kansas City; USA
<i>A. niger</i> P2	<i>A. niger</i> A1144 ptrA <sup>R</sup> , AoPamyB:terR:terR <sup>T</sup>	Gressler et al., 2015a
<i>A. niger</i> melA <sup>OE</sup>	<i>A. niger</i> A1144 ptrA <sup>R</sup> , AoPamyB:terR:terR <sup>T</sup> ; ble <sup>R</sup> , AtPterA:melA:AttrpC <sup>T</sup>	this study
<i>A. niger</i> his_melA <sup>OE</sup>	<i>A. niger</i> A1144 ptrA <sup>R</sup> , AoPamyB:terR:terR <sup>T</sup> ; ble <sup>R</sup> , AtPterA:his_melA:AttrpC <sup>T</sup>	this study
<i>A. niger</i> tyrP <sup>OE</sup>	<i>A. niger</i> A1144 ptrA <sup>R</sup> , AoPamyB:terR:terR <sup>T</sup> ; hph <sup>R</sup> , AtPterA:tyrP:AttrpC <sup>T</sup>	this study
<i>A. niger</i> tyrP:tdTom <sup>OE</sup>	<i>A. niger</i> A1144 ptrA <sup>R</sup> , AoPamyB:terR:terR <sup>T</sup> ; hph <sup>R</sup> , AtPterA:tyrP:tdTomato:AttrpC <sup>T</sup>	this study
<i>A. niger</i> melA <sup>OE</sup> tyrP <sup>OE</sup>	<i>A. niger</i> A1144 ptrA <sup>R</sup> , AoPamyB:terR:terR <sup>T</sup> ; ble <sup>R</sup> , AtPterA:melA:AttrpC <sup>T</sup> ; hph <sup>R</sup> , AtPterA:tyrP:AttrpC <sup>T</sup>	this study
<i>A. fumigatus</i> ATCC46645		ATCC; Manassas; USA
<i>A. fumigatus</i> $\Delta$ pksP	<i>A. fumigatus</i> ATCC46645 pksP <sup>-</sup> (UV mutant)	(Jahn et al., 1997)
<i>A. nidulans</i> SCF1.2	veA1	(Fleck and Brock, 2008)
BL21(DE3) Rosetta2	fhuA2 [lon] ompT gal ( $\lambda$ DE3) [dcm] $\Delta$ hsdS $\lambda$ DE3 = $\lambda$ sBamHI $\Delta$ EcoRI-B int::(lacI::PlacUV5::T7 gene1) i21 $\Delta$ nin5 with plasmid pRARE2	Novagen, Germany
BL21(DE3)_tyrP++	BL21(DE3) Rosetta2 genotype with PT7:tyrP++- pET43.1H6	this study
BL21(DE3)_tyrP+	BL21(DE3) Rosetta2 genotype with PT7:tyrP+- pET43.1H6	this study

## Supplemental Experimental Procedures

### Gene deletion and complementation in *A. terreus*

Gene deletion constructs were generated by PCR amplification of 0.5 – 1 kb upstream and downstream flanks of the gene of interest using Phusion Hot Start II polymerase (Thermo Scientific, Braunschweig, Germany) and genomic DNA from *A. terreus* SBUG844 as template. Oligonucleotides P21-P44 were used for the specific gene deletions and are shown in supplemental table of oligonucleotides. Deletion constructs generally contained the *ptrA* resistance cassette (Fleck and Brock, 2010) and were assembled by *in vitro* recombination (InFusion Enzyme Mix, Clontech, Saint-Germain-en-Laye, France) in a *KpnI*-linearised pUC19 vector by mixing the plasmid with the resistance cassette and the two gene specific flanks. Plasmids were amplified in *E. coli* DH5 $\alpha$  and re-isolated using the NucleoSpin Plasmid (Machery-Nagel, Düren, Germany). Deletion constructs were excised by *KpnI* restriction and used for transformation of the *A. terreus* SBUG844/ $\Delta$ *akuB* strain (Gressler et al., 2011). The *mela* deletion was complemented using P29 and P45-47 and *tyrP* deletion with P33 and P48, 49 and P36. Complementation constructs consisted of the entire coding region including the upstream flank and a short terminator sequence, the phleomycin resistance cassette and a downstream flanking region that were assembled by *in vitro* recombination.

### Heterologous gene expression in *Aspergillus* species

Cloning of *mela* in SM-Xpress was performed with oligonucleotides P64-P71 and resulted in *A. niger* strain *mela*<sup>OE</sup>. An *N*-terminally His-tagged MelA was produced with oligonucleotide P72 and P81, the former oligonucleotide containing a His-tag coding sequence. The amplified product was cloned into the SM-Xpress vector. The *tyrP* gene was amplified with P73/74 and cloned into the *NsiI* restricted His\_SM-Xpress vector to add a *C*-terminal His-tag. Subsequently, the phleomycin resistance cassette was replaced by the *NotI* restricted *hph* gene that derived from plasmid *hph\_pCRIV* (Fleck and Brock, 2010). Constructs were used for transformation of *A. niger* P2, *mela*<sup>OE</sup> or *A. terreus* SBUG844. For localisation studies of TyrP a *C*-terminal fusion with the red fluorescent protein tdTomato separated by a synthetic peptide linker sequence of 14 amino acids (QSTVPRARDPPVAT: (Mezzanotte et al., 2014)) was performed. The *tyrP* gene was amplified with oligonucleotides P75/76 and tdTomato gene with P77/78. All fragments were fused by *in vitro* recombination and used for transformation of *A. niger* P2 and *A. niger mela*<sup>OE</sup>.

### Generation the SM-Xpress2 and *his*\_SM-Xpress cloning vectors

To construct a vector that allows transformation of strains already carrying a SM-Xpress vector construct, the SM-Xpress2 vector was generated that contained the hygromycin B resistance cassette rather than the phleomycin cassette. Cloning of the gene of interest requires linearization with *NcoI* and an internal *NcoI* restriction site in the *hph* gene had to be removed. This was done by overlap PCR using primer pairs P56/57 and P58/59, which resulted in a silent point mutation. Subsequently, the *ble* gene was excised from SM-Xpress by *NotI* restriction and replaced by the mutated *hph* gene by *in vitro* recombination resulting in SM-Xpress2. For generating a vector suitable for production of His-tagged proteins a strategy was selected that allows either *N*- or *C*-terminal tagging of proteins in dependence of the restriction enzyme used for plasmid linearization. The *terA* promoter was amplified with oligonucleotides P60/61, which resulted in a 817 bp fragment with a 5'-overlap to the *EcoRI* restricted pUC19 vector and a His-tag sequence at its 3'-end. The *trpC* terminator was amplified with oligonucleotides P62/63 resulting in a 5'-overlap to the His-tag sequence and a 3' overlap to the resistance cassette. The promoter and terminator sequences were removed from the original SM-Xpress vector by *EcoRI* restriction and replaced by the new fragments *via in vitro* recombination. This resulted in plasmid *his*\_SM-Xpress that flanks the His-tag sequence 5' by an *NsiI* and 3' by an *NcoI* restriction site. This allows to tag proteins at the *C*-terminus by insertion of the gene of interest in the *NsiI*, whereas insertion into the *NcoI* restriction site results in a protein with an *N*-terminal His-tag.

### Purification of recombinant MelA

For purification of MelA an *A. niger* strain producing MelA with an *N*-terminal His-tag (P2\_*his-mela*) was selected. The strain was grown for 26 h at 30°C on 2  $\times$  100 ml YM medium. Mycelium was harvested over filter gaze (Miracloth, Merck, Darmstadt, Germany) and pressed dry. Approximately 4 g mycelium (wet weight) were ground to a fine powder under liquid nitrogen and suspended in buffer A (50 mM Tris-HCl, 150 mM NaCl, 10% glycerine at pH 7.5) supplemented with 20 mM imidazole. Cell debris was removed by 10 min centrifugation at 4°C and 14000  $\times$  g. The supernatant was filtered over a 0.45  $\mu$ m filter (Sartorius) before applied to a 1 ml Ni-Sepharose FF gravity flow column (Macherey-Nagel) previously equilibrated with the suspension buffer. After washing the column with 6 column volumes of buffer A containing 40 mM imidazole, MelA was eluted in buffer A with 200 mM imidazole. Eluates were concentrated and desalted against buffer A by use of centrifugal filter devices (Millipore, cut-off 30 kDa). Purity of the protein was checked by using Novex NuPAGE 4-12% Bis-Tris gels in a MES buffered running system (Invitrogen/Life Technologies/Thermo Scientific).

### Purification of recombinant TyrP from *A. niger* and *A. terreus*

Recombinant TyrP was purified from *A. niger* *tryP*<sup>OE</sup> and *A. terreus* PterA:*tyrP*<sup>++</sup> 10. The protein from both sources contained a C-terminal His-tag for purification via Ni-Sepharose. In an initial attempt *A. niger* *tryP*<sup>OE</sup> was grown for 36 h on AMM(-N)G100Gln50 medium and purification from ground mycelium was performed over Ni-Sepharose as described for purification of MelA from *A. niger*. Unfortunately, most of TyrP activity eluted at the 40 mM imidazole washing step and analysis by SDS PAGE did not allow unambiguously attributing a specific protein band to TyrP activity. Due to indications for a post-translational modification by glycosylation the purification procedure was adapted accordingly. First, enzyme production from *A. niger* was optimised by incubating the production strain for 36 h at 28°C in AMM(-N)50Gln with 2% soluble starch (Difco, Oxford, UK) as carbon source and 10 g/l talc (Sigma, Gillingham, UK). *A. terreus* was cultured for 28 h at 37°C in GSMY medium. From both species approximately 10 g mycelium (wet weight) was ground to a fine powder and suspended in 30 ml buffer B (20 mM Tris/HCl, 200 mM NaCl; pH 7.4). The suspension was centrifuged at 14,000 × g and filtered over 0.45 µm syringe filters. The cell-free extract was loaded on a 2 ml gravity-flow ConA-Sepharose 4B column previously equilibrated with buffer B. The column was washed with 3 column volumes of buffer B followed by 3 column volumes of a stringency wash with buffer B containing 50 mM methyl-α-D-glucopyranoside (Sigma). Elution was performed in buffer B with 1 M methyl-α-D-glucopyranoside. Elution was paused several times for about 15 min to increase elution efficiency (Soper and Aird, 2007). About 28 ml of active fractions were pooled and concentrated using a centrifugal filter device with a 30 kDa cut-off. Concentration of methyl-α-D-glucopyranoside was reduced by diluting the enzyme concentrate in buffer A and the solution was applied to a 1 ml gravity-flow Ni-Sepharose column. The column was washed with 4 column volumes buffer A containing 20 mM imidazole and TyrP was eluted by increasing the imidazole concentration to 200 mM. Enzyme purity was analysed by SDS-PAGE on Novex NuPAGE 4-12% Bis-Tris gels using a MES buffered running system.

### Purification of different TyrP versions from *E. coli*

For purification of proteins from *E. coli* Express Instant TB medium (Merck, Novagen) was used. Cultures of 20 ml were inoculated with BL21(DE3) Rosetta 2 cells carrying pET expression vectors with either the full length or truncated version of *tyrP*. *E. coli* cells were incubated at 28°C for 26 h or at 21°C for 40 h with identical results. Samples were disrupted by sonication and soluble and insoluble fractions were analysed for tyrosinase activity and for protein production via SDS-PAGE analysis. Since no activity was detected and the protein was exclusively detected from inclusion bodies, purification was performed under denaturing conditions. Approximately 0.5 g of cells were suspended in buffer A and disrupted by sonication (3 × 2 min continuous sonication at 60% power; Soniprep 150, MSE, London). Insoluble material was collected by centrifugation at 13,000 × g and washed once with buffer A. The pellet was dissolved for 30 min in 2 ml buffer C (50 mM Tris/HCl, 150 mM NaCl, 8 M Urea; pH 7.5). After centrifugation at 13,000 × g for 6 min the supernatant was loaded on a 1 ml Ni-Sepharose and washed with 6 ml buffer C with 20 mM imidazole followed by 5 ml with 40 mM imidazole. Proteins were finally eluted by increasing the imidazole concentration to 200 mM in buffer C. Purification was analysed by SDS-PAGE on Novex NuPAGE 4-12% Bis-Tris gels using a MES buffered running system.

### Isolation and characterisation of aspulvinones

Semi-preparative isolation of aspulvinones was performed on an Agilent 1260 series equipped with DAD and quaternary pump as described in the supplemental experimental procedures. Separation was carried out on a C18 column (Zorbax Eclipse XDB-C18, 5 µm, 250 × 9.4 mm, Agilent Technologies, Waldbronn, Germany) using a gradient of solvents A (water + 0.1% formic acid) and B (methanol). The following gradient was applied at a flow rate of 3.5 ml/min: 0 - 0.5 min 45% B, 0.5 - 4 min to 55% B, 4 - 16 min to 62% B, 16 - 19 min to 90% B, 19 - 19.5 min to 100% B holding to 26 min. Regeneration to 45% B from 26 - 30 min. Extracts from *A. terreus*  $\Delta$ *tyrP* were pre-fractionated using a SPE C18 cartridge (C18<sub>ec</sub>, Chromabond, Macherey and Nagel). The 60% MeOH portion containing Aspulvinones were used for semi-quantitative HPLC.

### H<sub>2</sub>O<sub>2</sub> sensitivity

Oxidative stress sensitivity was determined as described previously (Maerker et al., 2005) by the size of inhibition zones formed in the presence of various amounts of H<sub>2</sub>O<sub>2</sub>. The assay was performed on square 10 × 10 cm petri dishes with 40 ml (AMM(-N)G50Gln10 medium containing 2% agar. Top agar (20 ml) was mixed with 3 × 10<sup>8</sup> conidia for *A. fumigatus* and 4 × 10<sup>8</sup> conidia for *A. terreus* and poured on top of the bottom agar. Four holes with 1 cm in diameter were punched and varying amounts of a 3% H<sub>2</sub>O<sub>2</sub> solution (25 µl to 100 µl) were added. Plates were incubated for 20 h at 37°C and inhibition zones were measured. All tests were performed in triplicates.



## Electron microscopy

For scanning electron microscopy conidia were collected directly from plates. Plates were point inoculated with *A. terreus* strains and incubated for 7 days at 37°C to yield colonies with mature conidiophores. Plates were turned upside down and conidia were transferred directly to the sample holder on an electrically conductive and adhesive tag (Leit-Tab, Plano GmbH, Wetzlar, Germany) by carefully tapping on the back of the plate. Conidia were fixed for 24 h in the vapour of a 1:1 mixture of formaldehyde and glutaraldehyde. A critical point drying was not performed. To avoid surface charging the samples were coated with platinum (thickness approx. 2 nm) by high vacuum evaporation using a BAF 400 D (BALTEC, Liechtenstein). Coated conidia were investigated with a field emission scanning electron microscope LEO-1530 Gemini (Carl Zeiss NTS GmbH, Oberkochen, Germany) at electron energy of 8 keV using the in-lens secondary electron detector and magnifications of 50,000 to 200,000×. For transmission electron microscopy conidia were harvested in sterile water, washed once and the pellet was overlaid with freshly prepared 0.1 M cacodylate buffer (pH 7.2) containing 2.5% glutaraldehyde and fixed for 2.5 h at room temperature. After washing three times with pure cacodylate buffer the pellet was post-fixed for 1 h with 1% osmium tetroxide and dehydration in ascending ethanol series followed by post-staining with uranyl acetate. Subsequently, the pellets were embedded in epoxy resin (Araldite) and ultrathin sectioned using a LKB Ultratome III (LKB, Stockholm, Sweden). After mounting on filmed Cu grids and post-staining with lead citrate the sections were studied in a transmission electron microscope EM 900 (Zeiss, Oberkochen, Germany) at 80 kV and magnifications of 3,000 to 20,000×.

## Germination analysis

Fluorescein isothiocyanate (FITC; Sigma) labelled conidia were used for germination analyses. Conidia were adjusted to 10<sup>6</sup> conidia per ml in PBS with 0.01% Tween. For germination analyses 10 µl of the respective conidia suspension were added to 790 µl PDB medium in four well chamber slides (NUNC, Thermo Scientific) and incubated for 8 h at 37°C and 5% CO<sub>2</sub>. Slides were centrifuged at 200 × g and the medium was carefully removed. Conidia were embedded in a mounting solution containing DAPI (ProLong Gold Antifade with DAPI; Invitrogen/Thermo Scientific), incubated over night at 4°C and the number of germinated and non-germinated conidia was counted using an AxioImager fluorescence microscope (Zeiss, Jena, Germany). Experiments were performed in triplicates and approximately 1000 conidia per strain were evaluated.

## Supplemental References

- Fleck, C.B., and Brock, M. (2008). Characterization of an acyl-CoA: carboxylate CoA-transferase from *Aspergillus nidulans* involved in propionyl-CoA detoxification. *Mol Microbiol* 68, 642-656.
- Fleck, C.B., and Brock, M. (2010). *Aspergillus fumigatus* catalytic glucokinase and hexokinase: expression analysis and importance for germination, growth, and conidiation. *Eukaryot Cell* 9, 1120-1135.
- Gressler, M., Zaehle, C., Scherlach, K., Hertweck, C., and Brock, M. (2011). Multifactorial induction of an orphan PKS-NRPS gene cluster in *Aspergillus terreus*. *Chem Biol* 18, 198-209.
- Hutner, S.H., Provasoli, L., Schatz, A., and Haskins, C.P. (1950). Some Approaches to the Study of the Role of Metals in the Metabolism of Microorganisms. *Proc Am Phil Soc* 94, 152-170.
- Jahn, B., Koch, A., Schmidt, A., Wanner, G., Gehringer, H., Bhakdi, S., and Brakhage, A.A. (1997). Isolation and characterization of a pigmentless-conidium mutant of *Aspergillus fumigatus* with altered conidial surface and reduced virulence. *Infect Immun* 65, 5110-5117.
- Maerker, C., Rohde, M., Brakhage, A.A., and Brock, M. (2005). Methylcitrate synthase from *Aspergillus fumigatus*. Propionyl-CoA affects polyketide synthesis, growth and morphology of conidia. *FEBS J* 272, 3615-3630.
- Mezzanotte, L., Blankevoort, V., Lowik, C.W., and Kaijzel, E.L. (2014). A novel luciferase fusion protein for highly sensitive optical imaging: from single-cell analysis to *in vivo* whole-body bioluminescence imaging. *Anal Bioanal Chem* 406, 5727-5734.
- Soper, A.S., and Aird, S.D. (2007). Elution of tightly bound solutes from concanavalin A Sepharose. Factors affecting the desorption of cottonmouth venom glycoproteins. *J Chromatogr A* 1154, 308-318.